Phase Behavior of Water and Cyclodextrin Systems

Markus Enekvist

Lund University
Department of Chemical Engineering LTH

February 2017

Supervisors: Stefan Ulvenlund and Vitaly Kocherbitov
Examiner: Marie Wahlgren

Abstract

The effect of water on α-, β-, and γ-cyclodextrins (CD) was investigated using sorption calorimetry, differential scanning calorimetry and dynamic vapor sorption in order to understand the phase behavior and to create phase diagrams. By relating earlier X-ray diffraction patterns of cyclodextrins equilibrated over saturated salt solutions and literature regarding the cyclodextrin hydrates to the sorption calorimetry and vapor sorption results, it proved possible to determine several distinct cyclodextrin structures depending on the cyclodextrin/water composition. For α-cyclodextrin, a phase diagram was derived, containing four distinct hydrates with a possibly stoichiometric hydrate at α-CD·6H_2O and a hydrate of unknown stoichiometry close to α-CD·11H_2O. For β-cyclodextrin, the suggested phase diagram has three distinct hydrates that are non-stoichiometric in nature, with the most hydrated form being β-CD·10-12H_2O. The γ-cyclodextrin was investigated with sorption calorimetry and compared to X-ray diffraction patterns, which suggested up to four separate hydrates. The structures were less crystalline at a lower humidity than the α- and β-cyclodextrin counterparts.

Preface and Acknowledgements

The experimental part of this master's thesis was performed in the Department of Biomedical Science at the faculty of Health and Society, Malmö University. This report is the final installment of my master's degree in Chemical Engineering with specialization Pharmaceutical Technology at the Faculty of Engineering LTH.

Without the help of my supervisor, professor Vitaly Kocherbitov, this thesis would not have been possible. I learned a great deal from working with him. The valuable advice given by Stefan Ulvenlund has also been of great importance.

I would like to extend a special thanks to the people working at the Biomedical Laboratory, their tips and feedback made the day-to-day work not only easier, but also more enjoyable.

I would also like to thank my fiancé Julia, and my Finnish Lapphund Luna for continuous encouragement during the process.

I hope to be able to work alongside all of you again in the future,
Markus

Contents

1. Introduction

The active ingredients and excipients in a solid formulation can reside in different structures. These structures can be highly varied in terms of their physiochemical and biopharmaceutical properties, which can affect the uptake and efficacy of the active pharmaceutical ingredient (API). Different cyclodextrins are widely used in the pharmaceutical industry, as well as cosmetics, the food industry, agriculture and chromatography.

Due to their torus shaped form with a circular cavity, the cyclodextrin molecules are prone to form inclusion complexes, mainly of the host-guest type, with other molecules. The non-cytotoxic nature, coupled with the host-guest interaction, is what makes the cyclodextrin useful as a solubilizer, chelating agent, and for chiral analytical methods. The most interesting of these abilities, at least in the context of this study, is their ability to form host-guest inclusion complexes. A guest molecule that is sterically able to be held inside the cavity of the cyclodextrin is provided a non-polar microenvironment without breaking or forming any covalent bonds. This relationship can improve the solubility of hydrophobic compounds, and offer protection from light, oxidation or other incompatible compounds. (Martin Del Valle 2004). Of the three first-generation cyclodextrins, α-, β-, and γ-cyclodextrin, β-cyclodextrin is generally the most used and economical of the three.

For an API to be effective, it needs to be sufficiently hydrophobic to cross the cellular membranes, but at the same time soluble enough to reach the membranes in the first place. Cyclodextrin has found use for compounds that cross the membranes as intended, but suffer from inferior drug delivery. As cyclodextrin only permeate membranes with difficulty, the accepted mechanism is that CD carries the pharmaceutical compound to the barriers by keeping them in solution, where the guest molecule can detach and diffuse through the membrane. Other methods to achieve solubility for hydrophobic APIs involve formulations with co-solvents, surfactants and altered pH conditions, which can cause adverse reactions, while cyclodextrins are largely devoid of harmful effects in reasonable doses. Other advantages in formulations with cyclodextrin include binding volatile compounds, increased stability of the API, reduction of smell, bitterness or irritation (Martin Del Valle 2004).

The main purpose of this thesis was to investigate how the structure of the three first generation cyclodextrins is affected by the water/cyclodextrin composition, compare it with earlier research, and create accurate and detailed temperature-composition phase diagrams for the α-, β-, and γ-cyclodextrin/water system. As far as the author of this thesis is aware, there is no readily available phase diagrams for either the α-, β- or γ-cyclodextrin/water systems

In order to study the crystal structures and amorphous state of the cyclodextrin the main methods were differential scanning calorimetry (DSC) and sorption calorimetry, with supportive use of dynamic vapor sorption (DVS), thermogravimetric analysis (TGA) and earlier X-ray diffraction (XRD) data.

2. Theory

2.1. Cyclodextrin

The cyclodextrin molecules are ring-shaped α-D-glucopyranose monomers linked by α(1-4) glycosidic bonds most commonly formed by six, seven or eight monomers, which are denominated α-, β-, and γ-cyclodextrin respectively. The β-cyclodextrin structure can be seen in figure 1. Smaller ring sizes would be too sterically strained, and cannot be produced by glycosyl-transferase enzymes, but other cyclodextrins with 10, 14 and 26 glucoses have been previously studied. The larger cyclodextrin rings, however, tend to lose the well-known "doughnut" shape found in α-, β-, and γ-CD (Szejtli 1998, Saenger 1998). A relevant property for the cyclodextrin to form inclusion complexes is the difference in hydrophilicity between the hydrophilic ring exterior, and the less hydrophilic inside. The result of this property is a favourable situation for a host-guest relationship with guest molecules that fit inside the cavity (Saenger 1998). An interesting difference between α-, β-, and γ-cyclodextrin, except for the difference in cavity size, is the variation in water solubility. While α-, and γ-cyclodextrin have a solubility of 0.15 M and 0.18 M respectively, β-cyclodextrin has a very limited solubility of 0.016 M at normal temperature and pressure (NTP) (Jozwiakowski 1985).

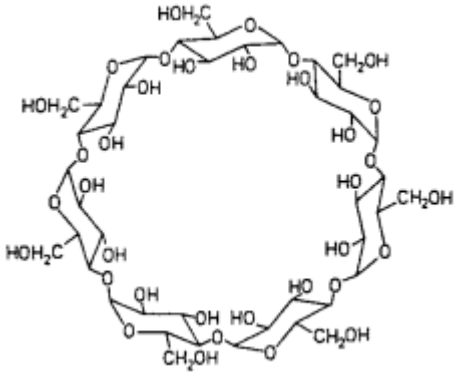

Figure 2. Chemical Structure of β-cyclodextrin (Saenger 1998).

In their solid state, cyclodextrin is known to form several different crystalline hydrates and crystal structures. The primary structures of cyclodextrins are either channel structures with linearly aligned cavities that form extended channels in the lattice as seen in figure 2 (c), or cage structures where the cyclodextrin is blocking off the nearby cavities, isolating the guest molecules. Typical cage structures are the herringbone and the brick structure, as can be seen in figure 2 (a) and (b). The channel type structure is stabilized by hydrogen bonding between the cyclodextrin molecules, and is normally found complexed with some small organic molecules, longer molecules, or ionic guests. The cage structures are more commonly found in cases where the α-, β-, or γ-cyclodextrins are co-crystallized with water or other smaller molecules. No crystalline forms of cyclodextrin devoid of guest molecules such as water have been reported (Saenger 1998).

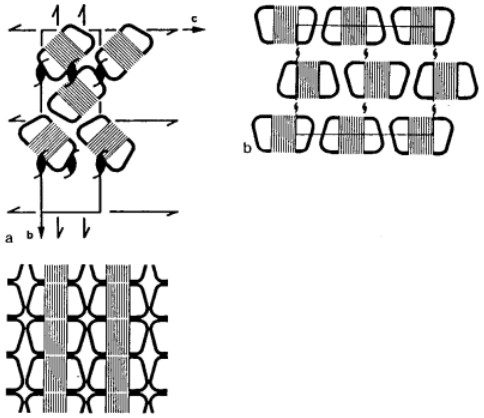

Figure 2. Schematic description of cyclodextrin in a (a) herringbone, (b) brick type, and (c) channel crystal structure (Saenger 1998).

Several single crystal structures of α-, β-, and γ-cyclodextrin have been reported, several with slight variations in water content. Some of the reported structures include α-CD·6H_2O (Klar 1980) α-CD·6H_2O (Manor 1974) and α-CD·11H_2O (Puliti 1998) for α-CD, with one paper specifying the hexahydrate as having four water molecules being located on the outer side of the cyclodextrin torus through extensive hydrogen bonding, and two water molecules located inside the cavity hydrogen bonded to each other and to the cyclodextrin (Manor 1974).

For the β-cyclodextrin, some of the determined structures include β-CD·11H_2O (Betzel 1984), β-CD·12H_2O [Lindner 1982], β-CD·10.5-12.0H_2O (Ripmeester 1993), β-CD·9.4-12.3H_2O (Steiner 1994), β-CD·8H_2O and β-CD·12H_2O, with the latter structure determined to have 6.5 water molecules statistically distributed over eight sites within the β-cyclodextrin cavity, and 5.5 water molecules statistically distributed over eight sites on the outside of the torus. The distribution is non-stoichiometric in nature, and all sites cannot be occupied by the water molecules at the same time due to steric hindrance (Lindner 1982). An investigation by Betzel/ et al found the same structure of eight water sites within the cavity and eight external sites, with 6.13 water molecules distributed over the former, and 4.88 water molecules distributed over the latter sites (Betzel 1984). This illustrates that the variation depending on methodology and other factors can be quite significant.

Some of the reported γ-cyclodextrin structures include γ-CD·13.3H_2O (Harata 1984), γ-CD·14.1H_2O (Harata 1987), and γ-CD·17H_2O (Maclennan 1980), displaying that some structures have been investigated several times with slightly different results. Like in β-cyclodextrin, the 14 sites in the cyclodextrin cavity, and the 9 external sites cannot be fully occupied due to steric hindrance, with 7.1 water molecules occupying the internal sites, and 7.0 water molecules occupying the outside for the tetradecahydrate of γ-CD (Harata 1987).

2.2. Phase Diagrams

According to Donald R. Askeland and Wendelin J. Wright a phase can be defined as any portion of a system that is physically homogenous within itself and bounded by a surface that separates it from other portions. An example of a system with several different and distinct phases could be solid ice, liquid water, and water vapor, which can all coexist in a stable system under certain conditions. An important relationship between the number of phases and number of components in a system is Gibbs phase rule:

$$2 + C = F + P$$

Here C is the number of chemically independent components, F is the number of degrees of freedom, and P is the number of phases present. The number 2 represents the ability to change pressure and temperature. However, as this thesis only considers phase diagrams with a fixed pressure, calculations of the degrees of freedom will use the number 1 instead. This study uses the two component cyclodextrin/water system in a temperature-composition diagram (Askeland 2014).

2.3. Differential Scanning Calorimetry

DSC is one of the more commonly used methods to measure the glass transition (T_g) and the melting temperature (T_m), but can also provide valuable information on heat capacity, crystallization, or other changes to a material. There are two different types of DSC. One type keeps a specific temperature or gradient by using individual heaters on two holders for hermetically sealed aluminium crucibles, one for the sample and one empty reference crucible, and measures the power difference. The other type (which is used in this thesis) is the heat flux DSC, which uses a single furnace and measures the temperature difference between the sample and the reference, which can be converted into the heat flow (Fried 2003).

2.4. Thermogravimetric Analysis

TGA is a method where changes in weight are measured as a function of an increase in temperature. The method can provide useful information regarding vaporization, desorption or several other physical or chemical changes. It relies on a furnace that can be controlled to increase the temperature steadily over time or hold it at a set temperature, and a precision balance for the sample. The TGA continually weighs the sample as it is heated, and the results are commonly plotted as a mass - temperature curve or a differential rate of mass loss - temperature curve (Coats 1963).

2.5. Dynamic Vapor Sorption

DVS is a technique focused on investigating the amount of water in a solid sample as a function of the water activity, called the sorption-desorption isotherm. The isotherm is divided into two separate curves, where the adsorption isotherm is created by increasing the humidity, and the desorption isotherm is created by decreasing the humidity. The difference between these two plots is called the hysteresis. Theoretically any volatile solvent could be used as vapor, but the most common application is water set between 0 percent relative humidity (%RH) and 100 %RH (Sheokand 2014).

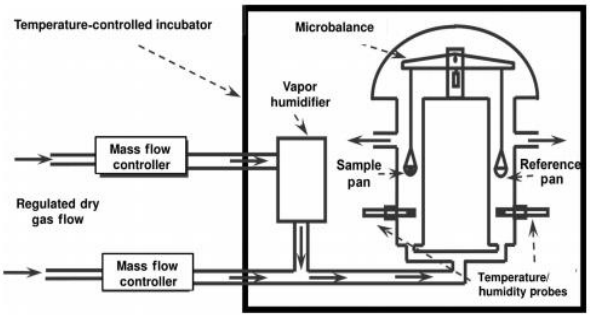

Figure 3: Schematic for a typical DVS instrument (Sheokand 2014).

Functionally, the DVS is a gravimetric method that contains a temperature controlled incubator with sample and reference chambers, a microbalance, and temperature and humidity probes. The mass flow controllers are programmed to create the desired humidity through the mixing of dry air and saturated vapor, an illustration of the instrument can be seen in figure 3.

2.6. Sorption Calorimetry

The isothermal sorption double twin calorimeter can provide useful information regarding the hydration of organic materials. Due to separate calorimetry measurements it can not only measure the sorption isotherm, but also the differential sorption enthalpy. The vessel itself has two chambers connected by a tube of known length and diameter. With the sample contained in one end of a vessel a vaporizable liquid, such as water, is added to the other end which will then vaporize and be adsorbed by the initially dry sample. The isothermal calorimeter measures the heat produced at a set temperature, and as the different chambers in the vessel are separated, they can also be separately monitored to provide the thermal power of evaporation P^{vap}, and the thermal power of sorption P^{sorp}. From these values registered in the upper and lower chamber it is possible to calculate the partial molar enthalpy of mixing of water:

$$H_w^{mix} = H_w^{vap} + P^{sorp}\frac{H_w^{vap}}{P^{vap}}$$

Where H_w^{vap} is the molar enthalpy of evaporation for water and H_w^{mix} refers to the molar enthalpy of mixing for water to CD, $H_2O(l) \rightarrow H_2O(CD)$. It is also possible to calculate the water activity in the sample chamber (Wadsö 2002, Kocherbitov 2011):

$$a_w = 1 - \frac{P^{vap}}{P_{\max}^{vap}}$$

2.7 X-Ray Powder Diffraction

While any XRD instruments have not been used for the duration of this study, an integral part of determining conformational changes in cyclodextrin is based on diffraction data derived from previous studies. X-ray diffraction can be used to provide information concerning the amorphous state, or the crystal structure of a crystalline material. The high energy photons (x-rays) targets a material, which results in a part of the beam being absorbed, and other parts scattered from electron interaction, which produces a scattering pattern. For a crystal the interplanar spacing and scattering angle can be connected by Bragg's law;

$$\sin\theta = \frac{\lambda}{2d_{hkl}}$$

Where θ is half the angle of the diffracted x-ray beam, and d_{hkl} is the interplanar spacing that cause constructive reinforcement of the x-ray beam. A powdered sample will for a given incident and reflected beam show these reinforced peaks, which can be used as a signature for a given crystalline material. (Askeland 2014, Fried 2003)

2.8. Non-freezing water

When a biopolymer is in a hydrated state, some of the water will interact with the polymer molecules. These water molecules are normally referred to as bound water. As the interactions between carbohydrates and water is normally weaker than the interactions between the water molecules themselves, cooling a hydrated biopolymer can almost fully dehydrate it by the crystallization of water. However, some of the water may stay in the biopolymer phase. The reason for this is an effect of water on the glass transition that prevents full dehydration. The water that stays in the biopolymer phase therefore does therefore not necessarily reflect the bound water at higher temperatures, and can be called the non-freezing water (Kocherbitov 2016).

3. Experimental

3.1. Materials and Data Handling

The α-cyclodextrin acquired from Wacker Chemie AG, and the β-, and γ-cyclodextrin was acquired from Sigma-Aldrich. The materials were dried, but otherwise used as received. The water added to the samples was ultrapure water by Veolia PURELAB.

Resulting data from the instruments were transferred to and processed in MathWorks MATLAB 2014b.

3.2. DSC

3.2.1. Sample preparation

The cyclodextrin samples were prepared by drying them under vacuum with molecular sieves for over 24 hours, after which they were transferred in a glove-box with <5 %RH into HPLC vials sealed with plastic paraffin film for storage. Over the course of the study, hydration of cyclodextrins was performed by several different procedures in order to find the most accurate and efficient method. These included:

- Adding 5-15 mg of dried α-cyclodextrin to an aluminium crucible of known weight and measuring the dry weight. The open crucibles were then transferred to desiccators, where they were equilibrated for over five days at constant temperature (21 °C) and humidity. The water activity in the desiccators was controlled through saturated salt solutions including $MgCl_2$, KCl, $Mg(NO_3)_2$, KNO_3 and NaCl. After removing the crucibles from the desiccators they were quickly sealed and weighed.
- Adding 10-20 mg of dried α-cyclodextrin to an aluminium crucible of known weight, and measuring the dry weight. A small amount of liquid water (approximately 3-15 mg) was then added before sealing the crucible. The samples were left to equilibrate for over two days before measurements were taken.
- Adding 100-200 mg dried α- or β-cyclodextrin to HPLC vials of know weight and measuring the dry weight. Purified water was added to reach a cyclodextrin mass fraction between 5 and 85 %. The HLPC vials were thoroughly mixed, and left to equilibrate for over five days. Before measurements were taken the vials were carefully mixed again in order to homogenize the fine cyclodextrin particles and ensure a representative sample was added to the aluminium crucibles.
- Carefully adding the base of the aluminium crucible to the DVS quartz sample pan and equilibrating it in the DVS at 0 %RH 25 °C until the mass was stable. A smaller amount of 2-5 mg dried α- or β-cyclodextrin was added and dried at 0 %RH 40 °C for one 45 minutes then equilibrated at 0 %RH 25 °C for 15 minutes. The relative humidity was set to an appropriate level for the intended hydration level, using earlier DVS data for 25 °C as reference. When the sample weight was within the desired range the program was stopped and the crucible was sealed as quickly as possible. Before DSC measurements the samples were left to equilibrate for over 24 hours.

3.2.2. DSC program

The DSC measurements were performed on a METTLER TOLEDO DSC-1 using STARe excellence software with Indium used for calibration. The sample was added to and weighed in a hermetically sealed aluminium crucible, and then lowered into the sample slot. The reference was an empty aluminium crucible weighing 49.00 mg. Sample purge flow of nitrogen was set to 80 ml/min and the nitrogen to the instrument was set to 240 ml/min. The program was started at -70 °C for 5 minutes, and then increased to the target temperature at a rate of either 1 °C/minute or 10 °C/minute.

3.3. Sorption Calorimetry

The sorption calorimetry experiments were conducted at 25 °C. The individual parts of the calorimetry vessel were cleaned with >99.5 % EtOH, dried with pressurized air, and placed in a desiccator with blue silica gel overnight under vacuum. The lower chamber was then cleaned in a plasma cleaner at RF level High for 5 minutes before assembly. The empty vessel was weighed a total of 5 times over 20 minutes. After drying the sample under vacuum with molecular sieves for over 24 hours, the α-, β-, or γ-CD samples were transferred to the upper chamber in a nitrogen gas flushed glove box with <5 % relative humidity. The vessel was then weighed a total of 5 times over 20 minutes again to get a stable mass of the sample. The injection channel was added to the vessel which was then carefully lowered into the calorimeter. When the baseline was stabilized, after approximately 24 hours, approximately 250 µl purified water was added to the lower cell.

3.4. DVS

The α- and β-CD samples were dried under vacuum with molecular sieves for over 24 hours before analyzing them on a TA Instruments Dynamic Water Vapor Sorption Analyzer Q5000 SA. The quartz crystal sample pans were cleaned with >99.5 % EtOH and dried with pressurized air before adding between 2-4 mg of the dried sample and starting the program. The samples were dried at 40 °C at 0 %RH for one hour, and then analyzed for adsorption/desorption between 0 %RH and 95 %RH at 25, 40, 50 or 60 °C. The rate of relative humidity increase was set to a step increment of 5 % RH per hour for α-cyclodextrin, and 1 %RH per hour for β-cyclodextrin in the range of 0-25 %RH with 5 %RH per hour for the remainder of the program.

3.5. TGA

The α- and β-CD samples were dried under vacuum with molecular sieves for over 24 hours before analysis on a TA Instruments TGA Q500 thermogravimetric analyzer. The samples were added to the platinum sample pan and heated under nitrogen gas from 20 °C to 800 °C at a heating rate of 10 °C/min.

4. Results and Discussion

4.1. α-cyclodextrin

4.1.1. Sorption Calorimetry and Dynamic Vapor Sorption

The sorption calorimetry data for α-cyclodextrin, as seen in Figure 4, show that there are three distinct one phase regions. The first one is between 1-2, second is 3-4 and the most hydrated region is 5-6. The corresponding water concentrations are between 0.66-1.34 %, 6.00-6.62 % and 8.94-9.94 %, respectively. All values for the α-cyclodextrin phase transitions can be found in Table 1 and Table 2. The method to calculate the regions for vapor sorption is illustrated in Figure 44 in Appendix 7.1, and the DVS regions was calculated through cubic spline interpolation. The most hydrated α-cyclodextrin structure is, according to the sorption calorimetry data, α-CD·6H_2O, which is consistent with the most commonly reported structure in literature [Manor 1974]. However, neither the sorption calorimetry nor the sorption isotherm created by DVS gave any evidence for the crystalline phase α-CD·11H_2O reported by Puliti et al. (Puliti 1998).

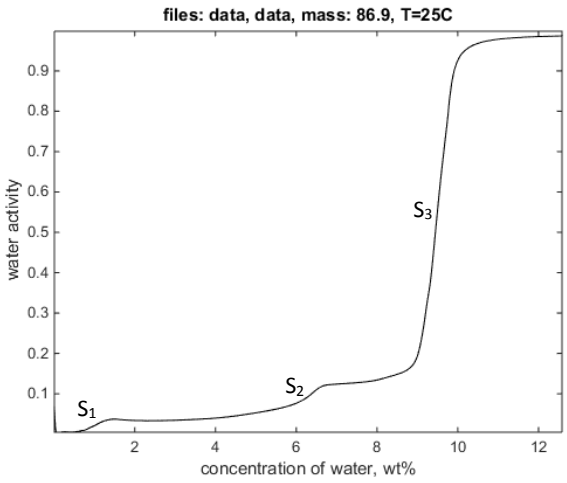

Figure 4. Sorption calorimetry data for α-cyclodextrin, sample size 86.9 mg. S_1, S_2 and S_3 denote the one phase regions seen in Table 1 and table 2.

The adsorption isotherm from the DVS data, as seen in Figure 5, has the same features, but the three one-phase regions have a water concentration between 0-0.21 %, 4.78-5.44 %, and 7.69-8.50 %water. These values are consistently and significantly lower than the sorption calorimetry comparison, but the overall appearance still remains the same.

Some possible reasons for the discrepancy between DVS and sorption calorimetry are differences in sample preparation. While the dried cyclodextrin was never exposed to air with a higher relative humidity than 5 %, the DVS procedure exposes it to air with >30 %RH for a longer period, up to a minute while loading the sample pan into the dry nitrogen flow. It is possible that the drying procedure in the DVS is less thorough than the 24-hour vacuum with molecular sieves, leaving more initial water in the samples. There are also other factors to consider when comparing the methods. Different techniques to measure the sorption isotherm may give slightly divergent results, as the measured isotherm will be influenced by factors such as the water transfer kinetics to and from the sample (Wadsö 2002).

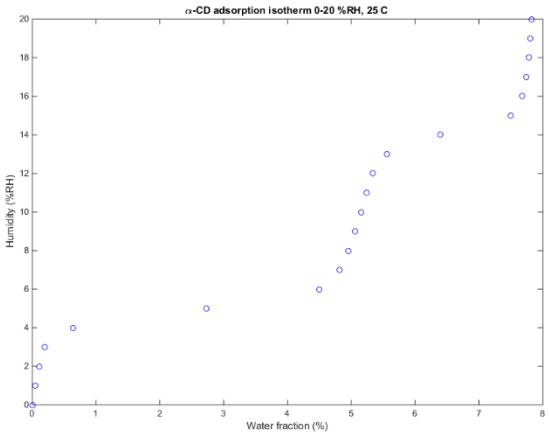

Figure 5. Adsorption isotherm for α-cyclodextrin from DVS between 0 and 20 %RH.

One additional calorimetry scan of α-cyclodextrin, which can be seen in Figure 44 Appendix 7.1, had a considerably less stable baseline, which could be attributed to some amount of water in the calorimetry cell. As a result, the first one-phase region is not distinguishable. The other regions are at equivalent positions as the ones in Figure 4, although at slightly lower water content, which is to be expected if the starting material is not properly dried. The remaining adsorption/desorption isotherms for α-cyclodextrin can be seen in Figure 6, and Appendix 8.1 Figure 45 and 46. Notable differences are the diminishing two phase regions, and higher measured water content for all regions. The latter phenomena could be explained by an increasingly dry starting material, as it is reasonable that the powder desorbs more water at 60 °C, 0 %RH than 40 °C, 0 %RH. The former change, however, appears to be a relevant as the intermediate one-phase region is between 0.66 percentage points (pp) wide at 25 °C, and is steadily increased to 1.3 pp at 60 °C, compare Figures 5 and 6.

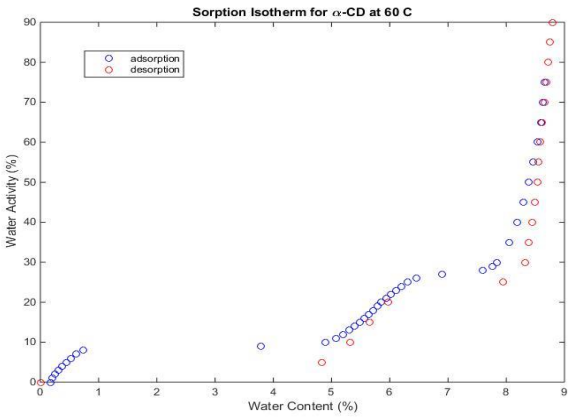

Figure 6. DVS data for the complete adsorption/desorption isotherm for α-cyclodextrin at 60 °C.

Table 1. The phase transitions measured by different temperatures and analysis methods. The results are presented as wt% of water, using the number connotation found in Figure 4, with S_x denoting different one phase regions.

Method	Temperature (°C)	S_1		S_2		S_3	
Sorp. Cal.	*25*	0.66	1.34	6.00	6.62	8.94	9.94
DVS	*25*	0	0.21	4.78	5.44	7.69	8.50
DVS	*40*	0	0.30	4.72	5.44	7.68	8.43
DVS	*50*	0	0.48	4.93	5.92	7.77	8.82
DVS	*60*	0	0.67	5.04	6.32	7.98	8.88

Table 2. The phase transitions measured by different temperatures and analysis methods presented in moles of water per mole of α-cyclodextrin

Method	Temperature (°C)	S_1		S_2		S_3	
Sorp. Cal.	*25*	0.36	0.73	3.45	3.83	5.30	5.96
DVS	*25*	0	0.11	2.71	3.11	4.50	5.02
DVS	*40*	0	0.16	2.68	3.11	4.49	4.97
DVS	*50*	0	0.26	2.80	3.40	4.55	5.22
DVS	*60*	0	0.36	2.87	3.64	4.68	5.26

Earlier vapor sorption experiments (Nakai 1986) have shown α-CD to be "dehydrated" down to less than one molecule of water per α-cyclodextrin, adsorb four molecules at 11 %RH, and having a maximum hydration at 6.6 water molecules per α-cyclodextrin over 79 %RH, see Figure 7. In order to dehydrate the α-cyclodextrin, Nakai et al. prepared it in at 110 °C for 3 hours under vacuum, which illustrates the difficulty of thorough dehydration. As will be elaborated on in the next section, their method of dehydration, however, produced a highly amorphous material that is completely different in XRD than the more crystalline anhydrate produced by drying in vacuum under molecular sieves.

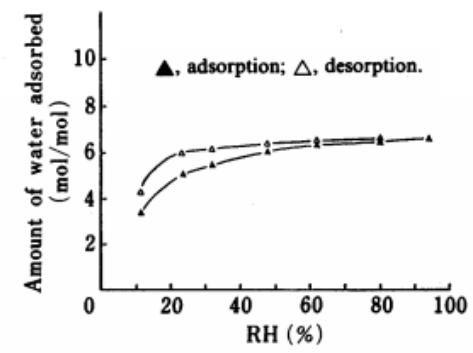

Figure 7. Water vapor sorption/desorption isotherm for α-CD 40 °C (Nakai 1986).

4.1.2. X-Ray Diffraction

In Figure 8, (a) represents the XRD pattern of the least hydrated structure, (b) the intermediate structure, and (c) the most hydrated structure of α-cyclodextrin. In comparison to Figure 9, the α-cyclodextrin dried at room temperature (left) has a distinctly different pattern from when it is dried at elevated temperatures (right). As the cyclodextrin stored at 11 %RH is still more amorphous, albeit slightly less than initially, than it is in the 21.6 %RH data, it suggests that the α-cyclodextrin does not properly recrystallize until it is stored at higher humidity levels. After recrystallization of the amorphous material at 79 %RH the diffraction pattern is very similar to the fully hydrated material, Figure 8 (c) and Figure 9 (c), clearly demonstrating that it re-crystallizes to the stable α-CD·6H_2O.

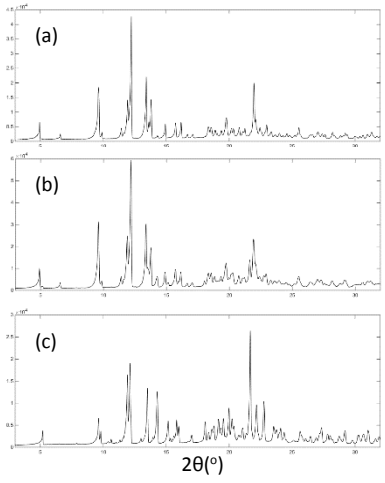

Figure 8. X-ray diffraction patterns for (a) 0 %RH (b) 21.6 %RH and (c) 97.3 %RH α-cyclodextrin. Data courtesy of Sanna Gustavsson et al.

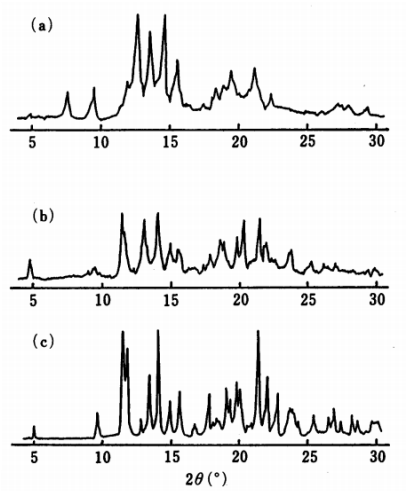

Figure 9. X-ray diffraction patterns for (a) dehydrated (b) 11 %RH and (c) 79 %RH recrystallized α-cyclodextrin (Nakai 1986).

The relevant α-cyclodextrin XRD measurements from Sanna Gustavsson et al. are shown in Figure 10. The diffraction patterns show little or no difference between the low humidity measurements at 0 – 11.3 %RH, seen in Figure 11. The same is true for the measurements between 32.8 and 97.3 %RH, as can be seen in Figure 12. No discernible peak-shift can be detected, so the compositional change of approximately 0.5 molecules of water per cyclodextrin when increasing the water activity does not seem to have any major effect on the crystal structure.

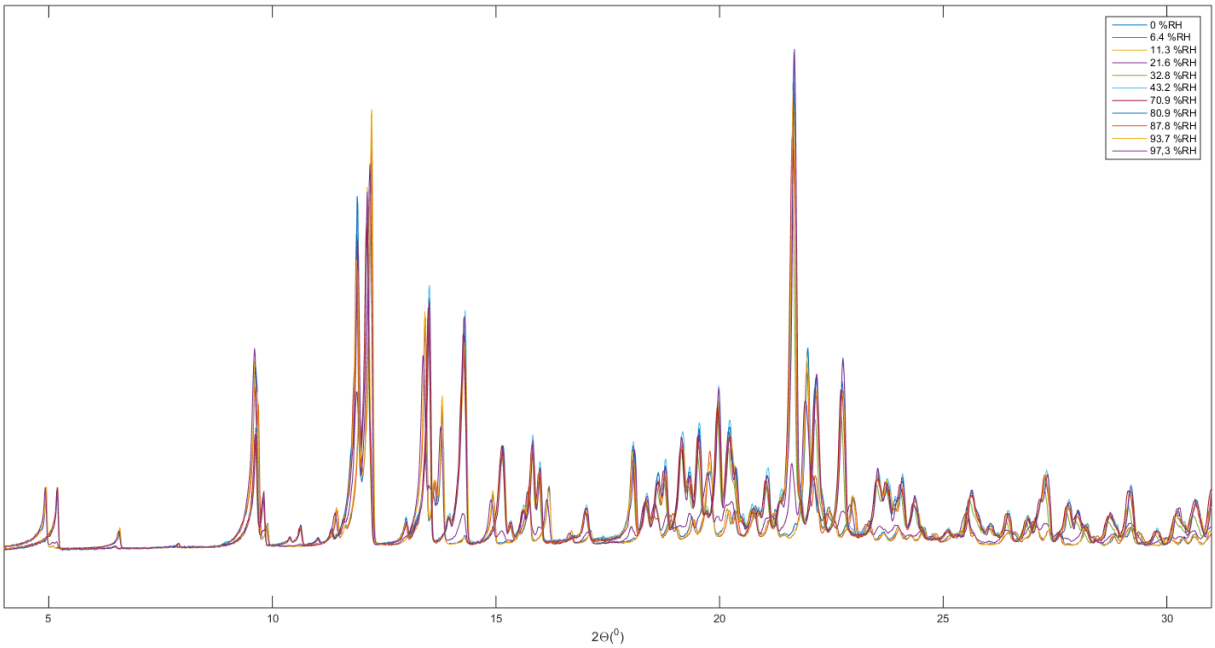

Figure 10. X-Ray diffraction patterns for α-cyclodextrin equilibrated in the humidity range 0-97.3 %RH.

All X-ray diffraction data presented has been normalized by the baseline between 7-7.5 degrees, and intensity normalized to the starting peak located at approximately 5 degrees.

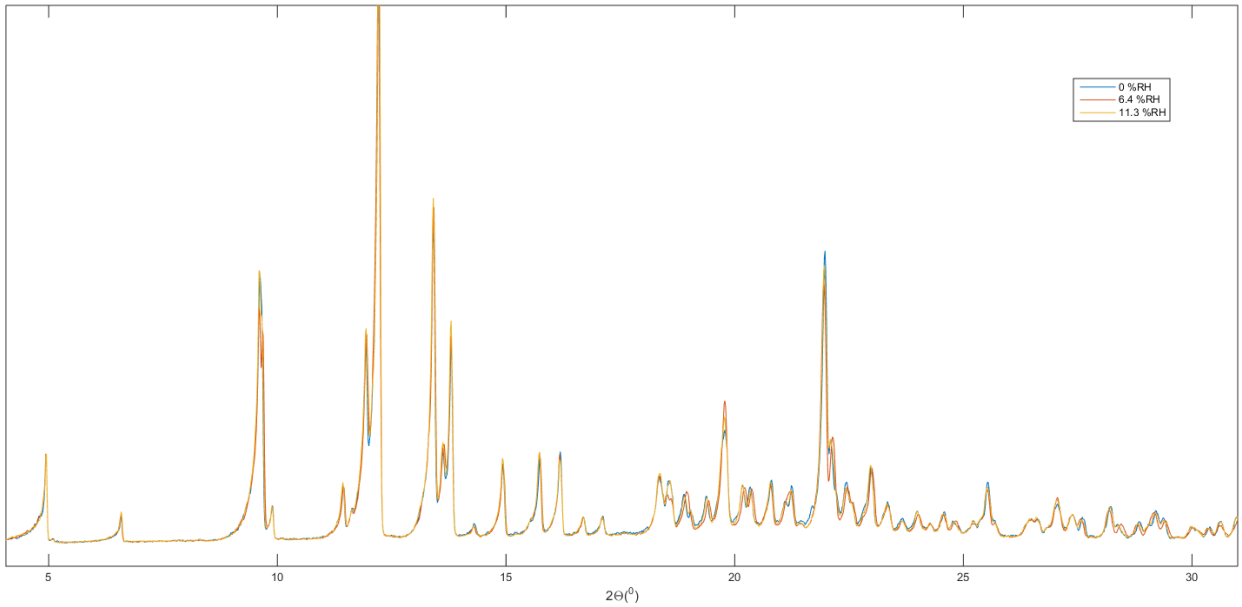

Figure 11. X-Ray diffraction patterns for α-cyclodextrin equilibrated at 0, 6.4 and 11.3 %RH.

The data in Figures 11 and 12 support the earlier calorimetry and sorption isotherm data, as there are no transitions over 30 %RH, meaning all scans between 32.8 and 97.3 %RH should be of the same, most hydrated, crystal structure. The scans between 0 and 11.3 %RH also appear to have the same structure, meaning the least hydrated crystal structure. The comparison between 11.3, 21.6 and 32.6 %RH seen in Figure 13 illustrates the transitions more clearly. There is a drastic difference between the 32.6 %RH diffraction pattern and the others, marking a clear transition. There is also, however, clear differences between 11.3 % and 21.6 %RH that cannot be found in other patterns in Figure 11. Notable differences are the peaks at 14.3°, 15.1°, 18.0° and 21.5°.

Even if the transitions in XRD are located at somewhat higher humidity than expected from sorption calorimetry and DVS measurements at 25 °C, it supports the notion that there are three crystal structures: one low hydration structure, one intermediate α-CD·4H_2O structure, and one well-established α-CD·6H_2O structure.

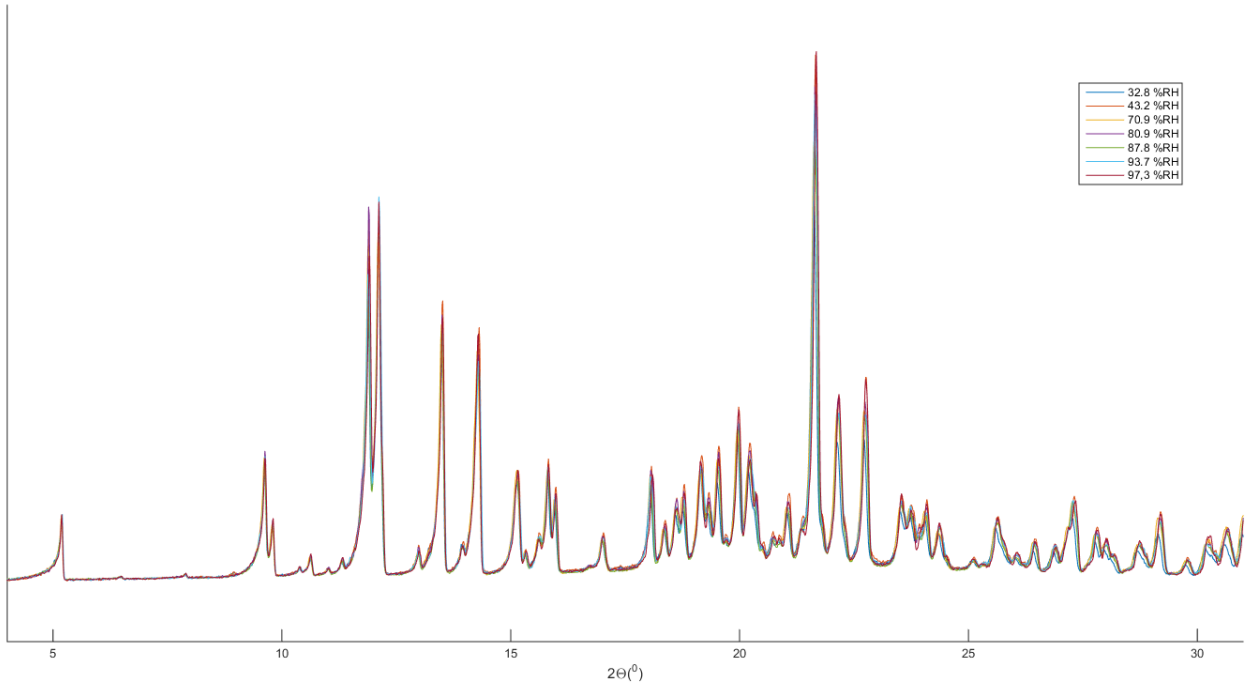

Figure 12. X-Ray diffraction patterns for α-cyclodextrin equilibrated between 32.8 and 97.3 %RH.

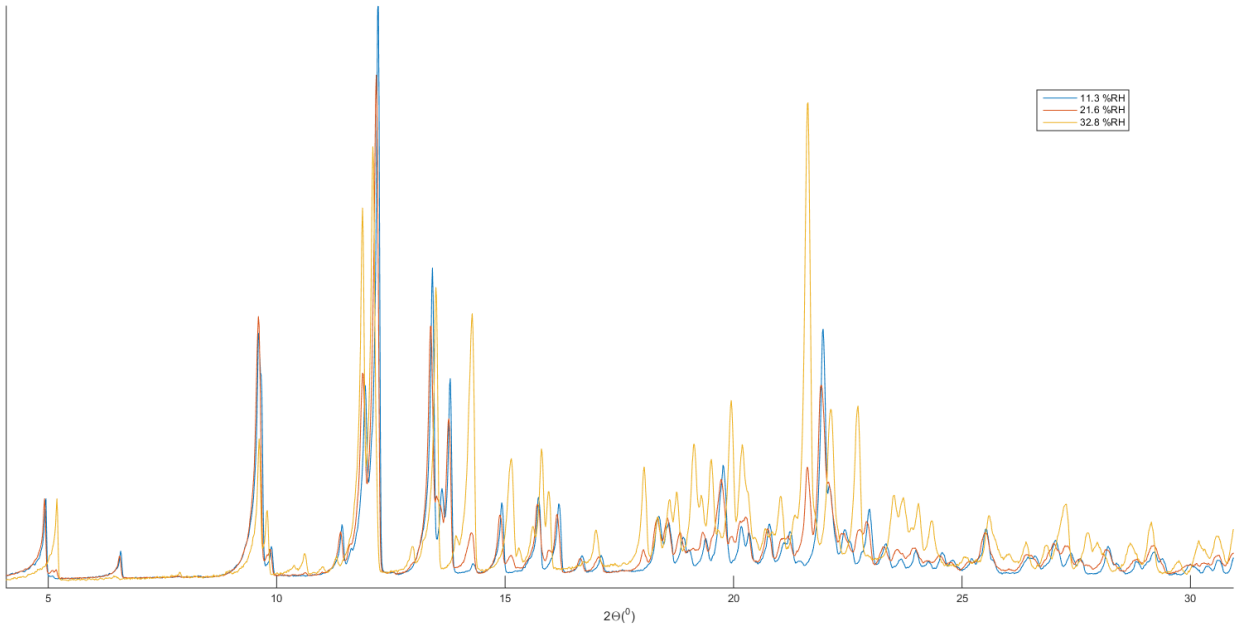

Figure 13. X-Ray diffraction patterns for α-cyclodextrin equilibrated between at 11.3, 21.6 and 32.6 %RH. All three patterns are assumed to represent different crystal structures.

4.1.3. Differential Scanning Calorimetry

For the α-cyclodextrin all of the DSC measurements were performed at 1 °C/minute, as the transitions were substantially more distinct at lower scan rates. Selected parts of the DSC scans are available in Appendix 7.1. The scans between 20.0 and 56.7 % cyclodextrin in water appear to show a transition from *liquid*+α-CD(*s*) → *liquid*. This is consistent both with the shape of the transition, as well as earlier literature (Specogna 2015). Due to the nature of the transition with a broad endothermic peak with a clear endset, the endset was used for temperature determination. In accordance with the dissolution data seen in Figure 14 from Specogna et al., 10 wt% α-cyclodextrin did not show any enthalpy change, as it was already fully dissolved. Their dissolution temperatures, however, are considerably higher for the other samples with a sharp, narrow transition, with a peak at 76.5 °C for 30 wt% α-cyclodextrin, see Figure 14. The start of an equivalent transition was found with a peak at 78.6 °C for 56.7 wt% α-cyclodextrin.

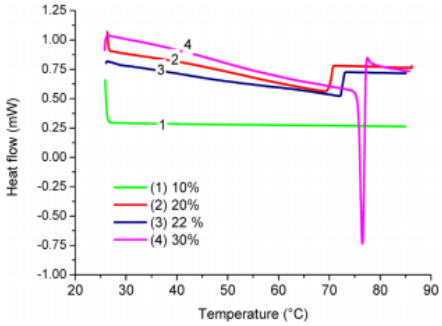

Figure 14. Heat flow of α-cyclodextrin at increasing concentrations (adapted from Specogna 2015).

Analysis of the heat flow between 20.0 and 91.9 wt% α-cyclodextrin can be seen in Figures 15,16 and 17. The transition temperature for dissolution was determined by the endset, and the transition temperature of the sharp peaks was determined by onset.

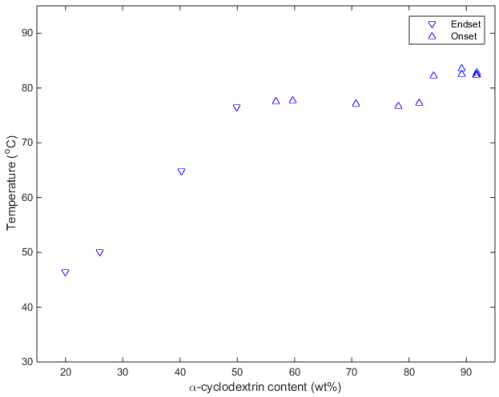

Figure 15. Onset and endset temperatures of peaks between 20 and 92 wt% α-cyclodextrin in water.

It is clear from Figure 15 that there are two distinct isothermal transitions: one with an onset of approximately 77 °C, and a second with an onset of approximately 82.5 °C.

The transition enthalpy increased linearly with the 77 °C isothermal transition, with an r^2 of 0.995. Extrapolation to 0 J/g gives a starting composition of 55.0 % α – cyclodextrin.

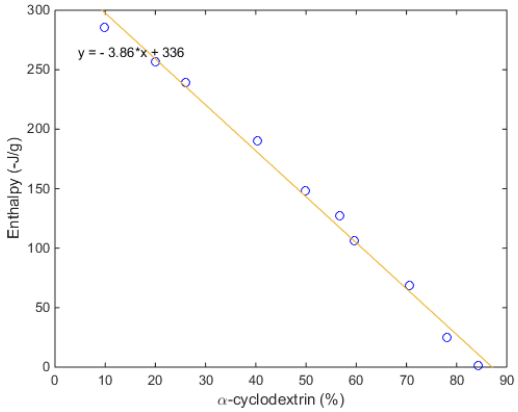

Figure 16. Enthalpy for the melting of ice at different α-cyclodextrin concentrations.

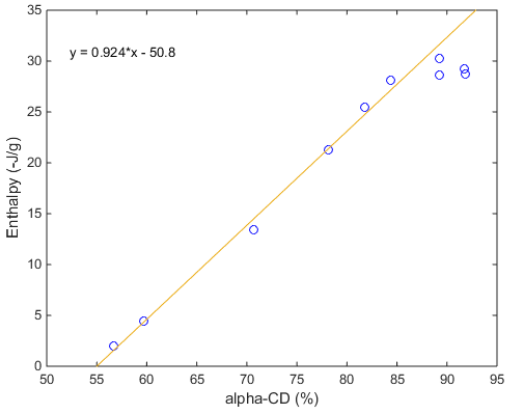

Figure 17. Enthalpy of the isothermal peaks seen in Figure 15. The linear regression is for the peaks between 0 and -25 J/g.

Another interesting comparison is the amount of freezing water in the samples. Figure 16 shows the relationship between the cyclodextrin content and water enthalpy, which is representative of the amount of freezing water. Linear regression extrapolates the amount of nonfreezing water to 13.0 %. The true amount, however, seems to be very close to the sample with 84.4 % α-cyclodextrin meaning that the nonfreezing water is closer to 15.6 % by weight. This is equivalent to α-CD·10H_2O.

While there was no visible indication by either sorption calorimetry or the sorption isotherm for a highly hydrated structure of α-cyclodextrin, the DSC scans show a change in the isothermal transition between 82 and 84 % α-cyclodextrin equivalent to between α-CD·10H_2O. and α-CD·12H_2O and the non-freezing water is equivalent to α-CD·10H_2O. These data, in combination with earlier reported crystal structures of α-CD·11H_2O (Puliti 1998), provide sufficient evidence to conclude that there is indeed a phase-transition from 82 to 84 % α-cyclodextrin, followed by a fourth one-phase region.

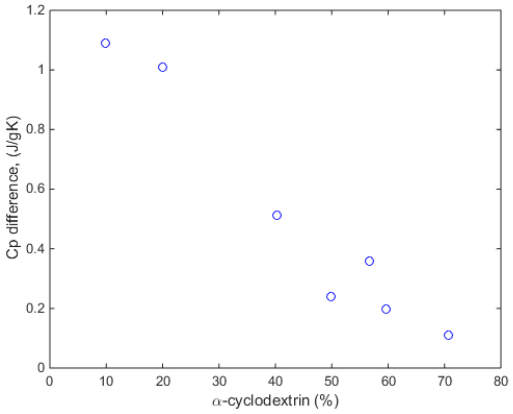

Figure 18. Enthalpy difference of the glass like transition for α-cyclodextrin.

One more interesting feature of the DSC scans in the 10 to 90 % α-cyclodextrin region is a possible transition with a consistent onset of -10 °C. The enthalpy is linearly diminishing with decreased water content, and not distinguishable over 75 % α-cyclodextrin, see Figure 18. It could possibly be a glass transition, but its exact nature is currently unclear.

The DSC scans in the range 93 to 100 % α-cyclodextrin are difficult to interpret. Some reoccurring features are endothermic peaks of highly varying enthalpy just over 30 °C, and a series of endothermic peaks between the intermediate and the least hydrated one phase region. The latter peaks have a temperature onset that decreases with increased α-cyclodextrin concentration, as can be seen in Figure 19, and linearly decreasing enthalpy, see Figure 20.

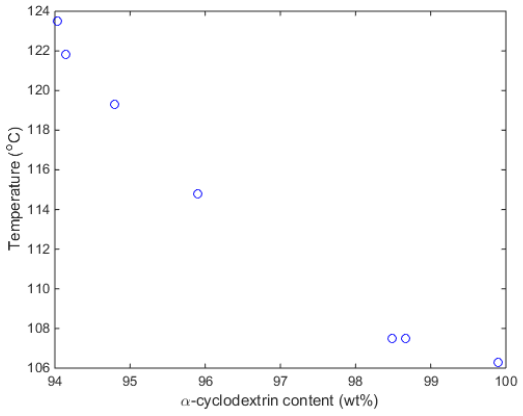

Figure 19. Onset temperature of the DSC peaks between 94 and 100 % α-cyclodextrin.

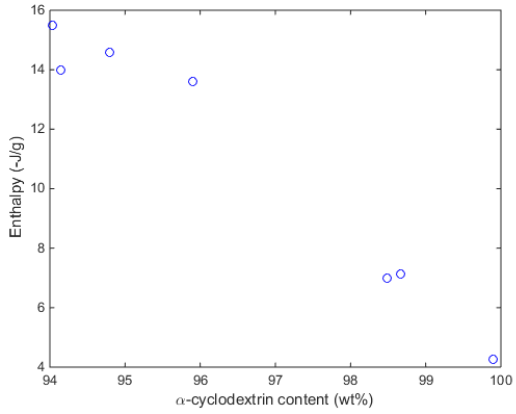

Figure 20. Enthalpy of the DSC peaks from Figure 19.

4.1.4. Adjustments for the α-cyclodextrin phase diagram

In order to derive a phase diagram for the α-cyclodextrin/water system, the discrepancy between the vapor sorption and the DVS sorption isotherm has to be addressed. The DVS isotherm is consistent with the vapor sorption isotherm data, but shifted to a lower water content. A likely explanation for this is the difference in drying of the α-cyclodextrin between the two methods; while the α-cyclodextrin for the vapor sorption is transferred into the chamber in a gloved box, the DVS exposes the powder to ambient air for up to a minute before the experiment is started. Because of this the DVS dries the α-cyclodextrin at 40 ^{o}C and 0 %RH for one hour, which is a less effective drying method than vacuum with molecular sieves. The DVS measurements will therefore be shifted by the difference between the DVS and the sorption calorimetry measurements at 25 ^{o}C in the phase diagram.

The only DSC peaks presented in the phase diagram are the ones who were deemed reproducible. There were, however, several additional events that could be of interest. These include endothermic peaks between 30-35 ^{o}C with high enthalpy variation, wide endothermic peaks between 55 and 75 ^{o}C in the S_2 region, and an endothermic peak at 60 to 70 ^{o}C for a sample equilibrated at 5 %RH.

4.1.5. Phase Diagram of α-cyclodextrin

The information obtained from sorption calorimetry, DVS and DSC was used to derive the phase diagram shown in Figure 21.

In Figure 21 S_1 to S_4 is designating the different solid forms of α-cyclodextrin. The isothermal transition of *liquid*+S_4→*liquid*+S_x could be melting of S_4, and starts at 55.0 wt% cyclodextrin as seen in Figure 16. The melted α-cyclodextrin will most probably be dissolved into the single phase liquid at increased temperatures, but that dissolution could not be found on DSC, either because the transition was not clear enough, or because it occurred at temperatures over 110 °C. The phase transition from S_3+S_4 →S_4+H_2O is set at α-CD·11H_2O in accordance with DSC data, non-freezing water and literature. Like S_1 S_2 and S_3 there is probably a one phase region for S_4, but it would need to be measured, for example using desorption calorimetry.

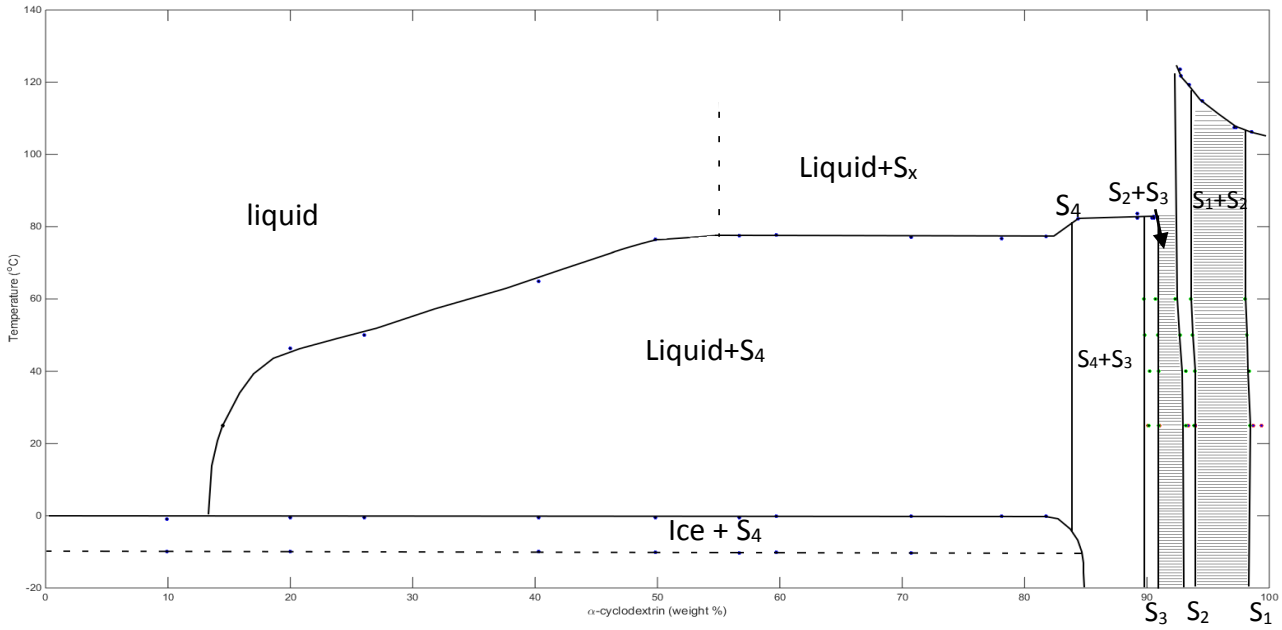

Figure 21. Temperature - composition phase diagram for the α-cyclodextrin/water system. Blue is DSC data, green is DVS data, red is sorption calorimetry data and black is the solubility at 25 °C (Jozwiakowski 1985).

4.2. β-cyclodextrin

4.2.1. Sorption Calorimetry and Vapor Sorption

Initially, some samples for the DSC were prepared by using saturated salt solutions. The weight-change of these samples could also be used to create a simple adsorption isotherm, that can be seen in Figure 22.

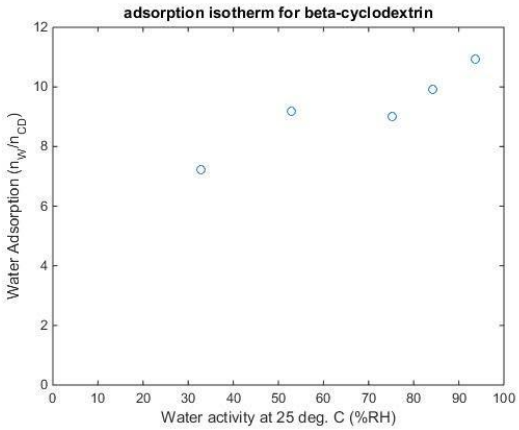

Figure 22. Adsorption for dried β-cyclodextrin equilibrated in saturated salt solutions.

As the adsorption isotherm from saturated salt solutions was lacking the details required to determine any solid phase transitions DVS seemed like a more effective option, which had the additional advantage of variable temperature. Figures 23-26 are the results from scanning dried β-cyclodextrin between 0 %RH and 95 %RH in steps of 5 % per hour.

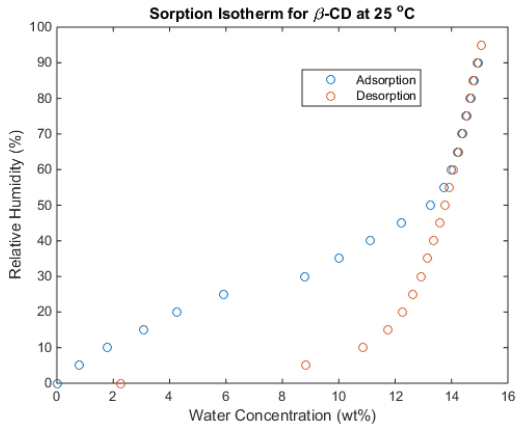

Figure 23. Sorption isotherm of β-cyclodextrin at 25 °C.

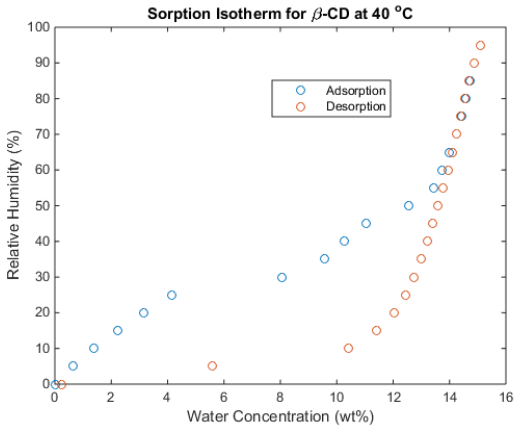

Figure 24. Sorption isotherm of β-cyclodextrin at 40 °C.

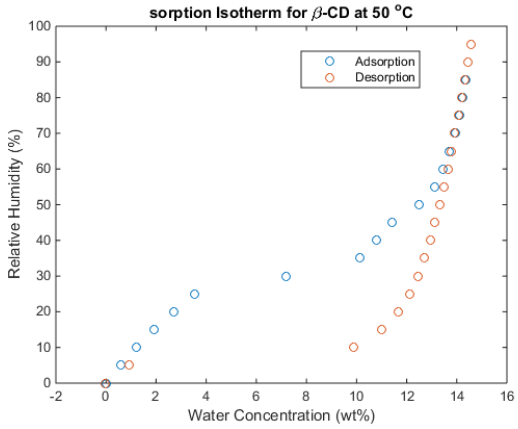

Figure 25. Sorption isotherm of β-cyclodextrin at 50 °C.

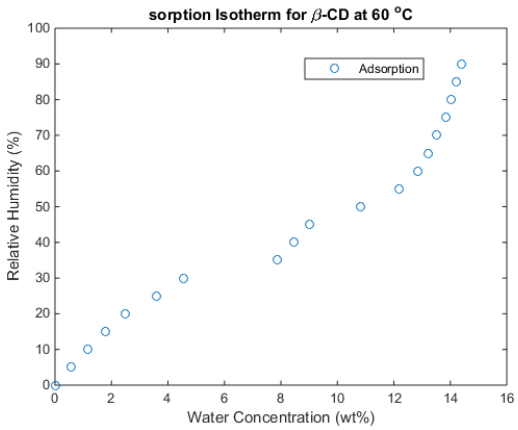

Figure 26. Adsorption isotherm of β-cyclodextrin at 60 °C.

While there is evidence of phase-transitions at all temperatures, the sorption isotherms at 40 and 50 °C have a significantly clearer two-phase region around 6 wt% water. One reason is that the vapor kinetics are too slow at lower temperatures, and the 25 °C adsorption isotherm would need longer than one hour per increment to equilibrate. A second two-phase region around 12 wt% water is only apparent in the sorption isotherm at 60 °C, but can also be detected in the sorption calorimetry measurements in Figures 27 and 28. The sorption calorimetry has the same two-phase regions that can be seen in the vapor sorption data, but also shows an irregular one-phase region up to 6 wt% water, with more even one-phase regions between 30 and 50 %RH and 55 to 95 %RH.

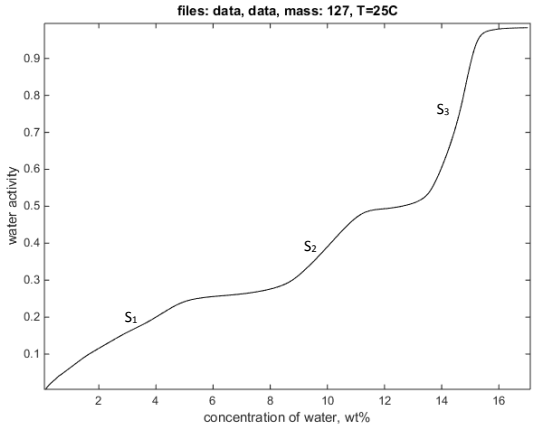

Figure 27. Sorption calorimetry scan of 127 mg β-cyclodextrin. S_1 S_2 and S_3 marks the one-phase regions for Table 3 and 4.

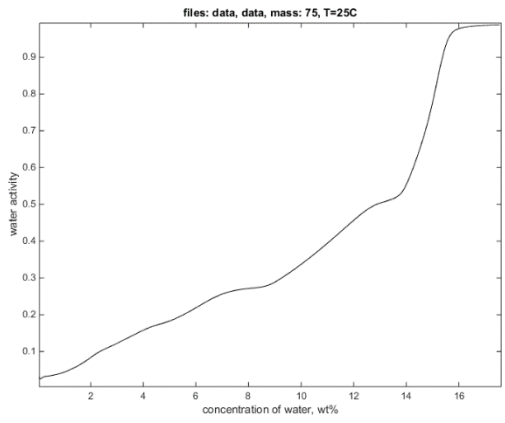

Figure 28. Sorption calorimery scan of 75 mg β-cyclodextrin.

All the discernible solid phase transitions can be seen in Table 3 and 4. In Table 3, the transitions are written as weight% water, while Table 4 lists them in number of moles of water per mole of β-cyclodextrin. All sorption calorimetry scans for composition and differential enthalpy are collected in Appendix 7.2.

Table 3. Solid state transitions between one- and two-phase regions in β-cyclodextrin, with data presented in weight percentage of water.

Method	Temperature (°C)	S_1		S_2		S_3	
Sorp. Cal.	25	0	4.69	7.93	10.83	13.18	15.11
Sorp. Cal.	25	0	4.98	8.58	11.14	13.44	15.30
Sorp. Cal.	25	0	7.07	8.78	12.59	13.84	15.65
DVS	25	0	5.16	-	-	13.54	15.22
DVS	40	0	4.66	8.82	11.23	13.36	15.24
DVS	50	0	4.30	9.57	11.58	13.62	14.71
DVS	60	0	3.76	7.60	9.40	12.98	14.83

Table 4. Solid state transitions between one- and two-phase regions in β-cyclodextrin, with data presented in moles of water per mole of β-cyclodextrin.

Method	Temperature (°C)	S_1		S_2		S_3	
Sorp. Cal.	25	0	3.1	5.4	7.7	9.6	11.2
Sorp. Cal.	25	0	3.3	5.9	7.9	9.8	11.4
Sorp. Cal.	25	0	4.8	6.1	9.1	10.1	11.7
DVS	25	0	3.4	-	-	9.9	11.3
DVS	40	0	3.1	6.1	8.0	9.7	11.3
DVS	50	0	2.8	6.7	8.3	9.9	10.9
DVS	60	0	2.5	5.2	6.5	9.4	11.0

As was the case with α-cyclodextrin, samples in DVS are slightly less hydrated than the sorption calorimetry measurements, probably due to the starting material for sorption calorimetry being slightly more dry. The difference is, however, not as pronounced for the β-cyclodextrin and most visible for the early transitions. Another interesting feature is that the S_2 region is significantly more varied than the S_1 and S_3 region.

4.2.2. X-Ray Diffraction

When comparing the diffraction patterns between 0 %RH and 33 %RH it is clear that the first and last patterns represent different structures. The transition, however, is not clear. The difference can be seen in Figure 29, and some gradually disappearing peaks are located at 6.5°, 9°, 13-14°, and 18°. The β-cyclodextrin patterns in Figure 29-32 were normalized by baseline between 7-8°, and intensity normalized for the 6° peak.

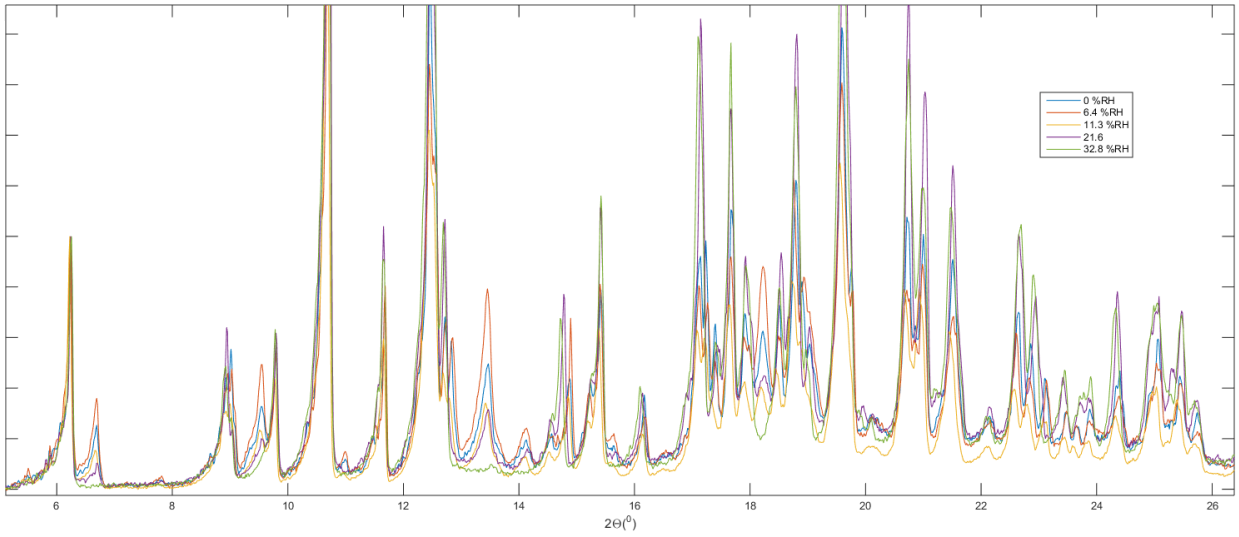

Figure 29. X-Ray diffraction patterns for β-cyclodextrin equilibrated between 0 and 32.8 %RH.

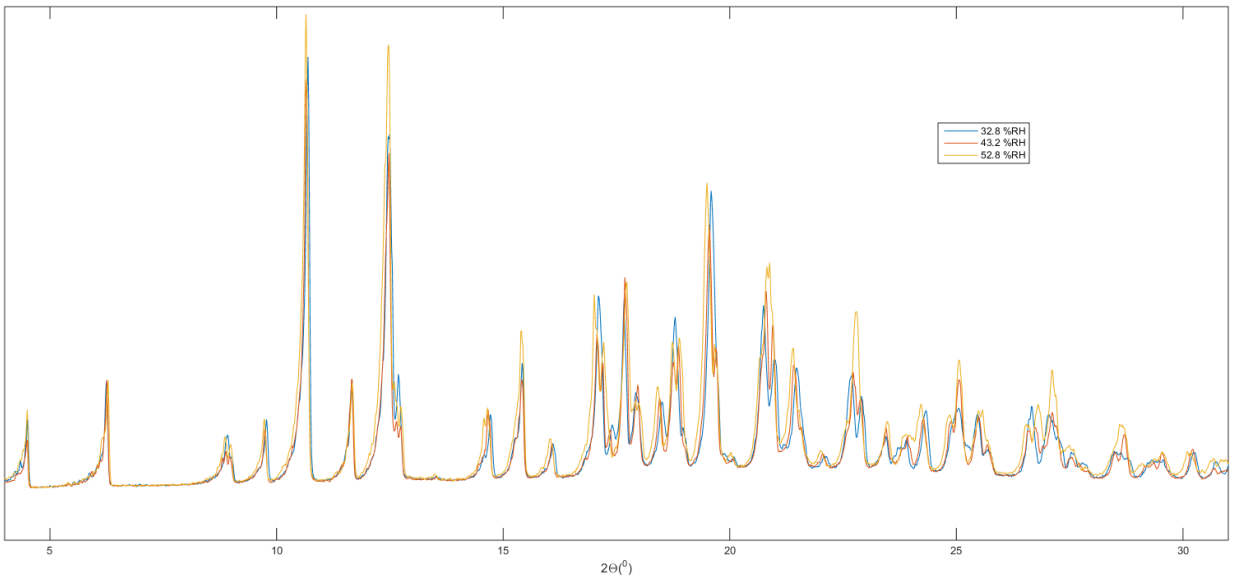

Figure 30. X-Ray diffraction patterns for β-cyclodextrin equilibrated between 32.8 and 52.8 %RH.

While the almost identical diffraction patterns for 32.8 %RH and 43.2 %RH are very similar to the diffraction pattern for 52.8 %RH and higher, there are some subtle differences at 21°, 23°, and in the 26-27° region. The diffraction data is somewhat inconclusive as regards a phase transition between 43 and 53 %RH, but does not disprove it.

For higher humidity levels, there were no clear differences between the diffraction patterns. Figure 31 illustrates the similarity from 52.8 %Rh to 97.3 %RH.

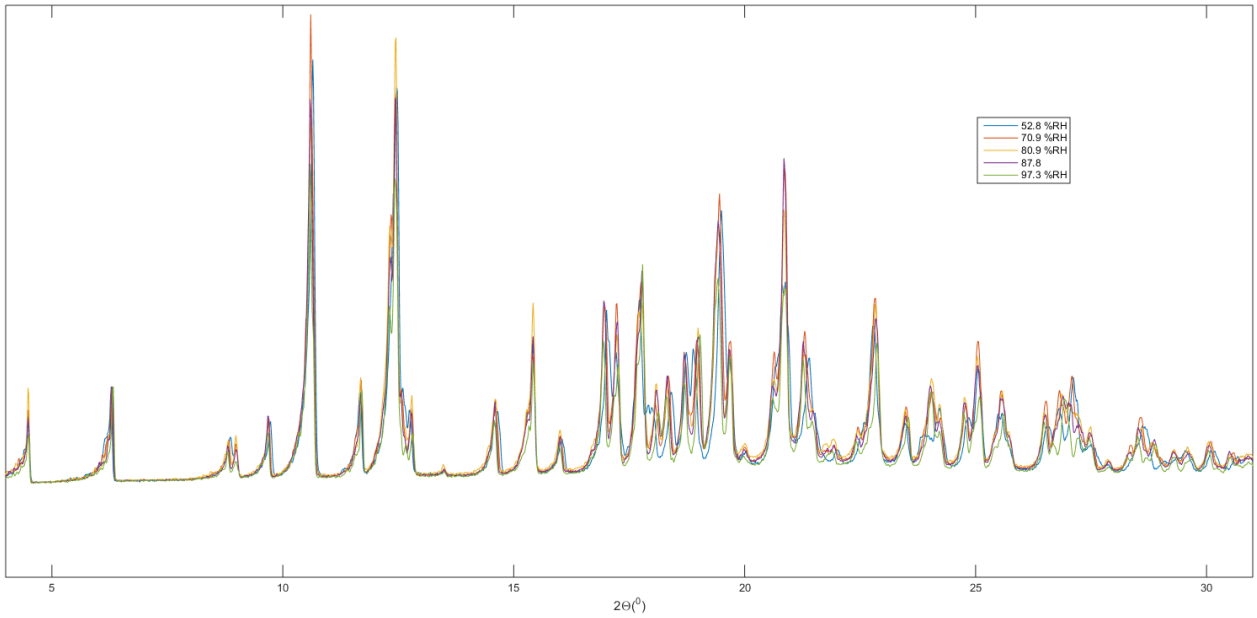

Figure 31. X-Ray diffraction patterns for β-cyclodextrin equilibrated between 52.8 and 97.3 %RH.

The sorption calorimetry and vapor sorption data show three one-phase regions of β-cyclodextrin hydrates. The first transition at roughly 25 %RH coincides with the largest difference in diffraction pattern, between 21.6 and 32.8 %RH. The gradual nature of the transition that is suggested by the step-by-step change of diffraction pattern is also reasonable when looking at the differential enthalpy from the sorption calorimetry that is not entirely consistent with a one-phase region. The second two-phase region is seen in calorimetry and vapor sorption at 50-55 %RH. While the diffraction pattern changes only marginally over that region, see Figure 32, the XRD, DVS and sorption calorimetry data together strongly suggest a second solid phase transition over the humidity region 50-55 %RH.

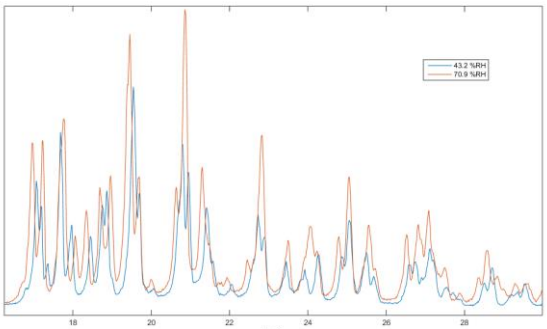

Figure 32. Diffraction pattern change for β-cyclodextrin between 43.2 and 70.9 %RH.

4.2.3. Differential Scanning Calorimetry

No thermally induced phase changes could be found for the β-cyclodextrin hydrates equilibrated over saturated salt solutions according to the DSC scans in Appendix 7.2. The crucible containing hydrated samples would rupture before any other deviations in the heat flow could be found, with a combined melting and chemical degradation at temperatures over 300 °C.

The β-cyclodextrin has quite low solubility at room temperature, at approximately 2 wt%. The solubility is improved at higher temperatures, and the heat flow showed a typical dissolution shape between 15 and 40 wt% β-cyclodextrin. As the DSC experiments at high water concentrations were limited to 110 °C in order to prevent the crucible from rupturing and to protect the instrument, no dissolution could be detected at higher concentrations. In comparison with MicroDSC measurements by Specogna et al., figure 34, the heat flow was very similar in shape but was the transitions were at lower temperatures for 15 and 20 wt% β-cyclodextrin.

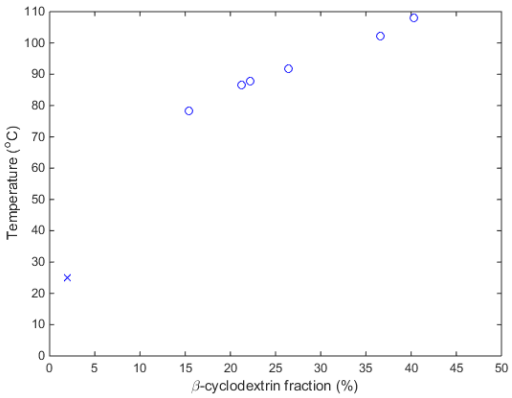

Figure 33. Endsets for the dissolution of β-cyclodextrin in water. (o) marks measured data, and (x) marks solubility at NTP.

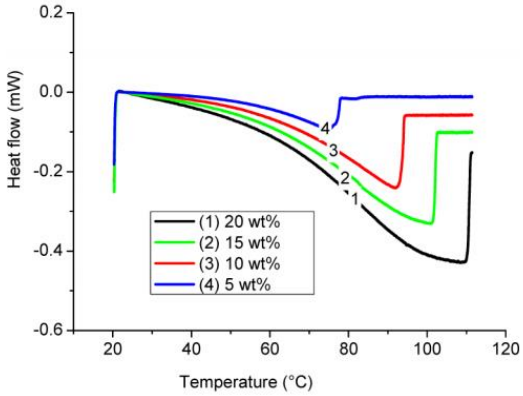

Figure 34. μDSC heat flow of β-cyclodextrin in water at different concentrations (adopted from Specogna 2015).

Measuring the melting enthalpy of the β-cyclodextrin/water system proved to be more complicated than initially thought. The early scans, seen in Figure 36, gave a very reasonable figure for the amount of nonfreezing water at β-CD·11.7H_2O, but the storage procedure of the dry β-cyclodextrin and β-cyclodextrin/water solutions were not optimal, which could affect the accuracy of measurement. A second set of samples were prepared with new storage procedures using short term storage in sealed HPLC vials. The resulting enthalpy measurements can be seen in Figure 35.

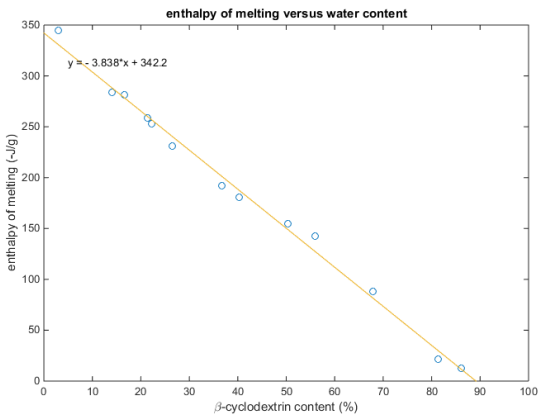

Figure 35. Second data set for the β-cyclodextrin/water system, with a nonfreezing water of 10.8 wt% water, or β -CD·7.6H_2O.

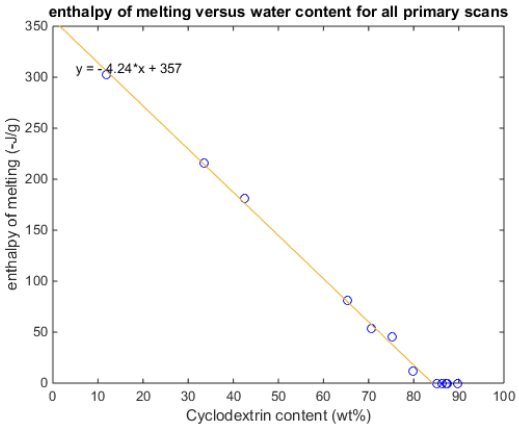

Figure 36. First data for β-cyclodextrin showing the nonfreezing water to be 15.8 wt%, or β-CD·11.7H_2O.

The resulting nonfreezing water of β -CD·7.6H_2O was lower than expected, so the dry β-cyclodextrin was tested in TGA and compared to another sample dried in an identical fashion. The first TGA scan indicated 7 moles of water per β-cyclodextrin molecule (Figure 37), while the second scan indicated less than 0.6 moles of water per β-cyclodextrin molecule (figure 38) remaining in the dried β-cyclodextrin. Due to the TGA method, the cyclodextrin will adsorb some water from the ambient air during the time it takes to start the heating program, somewhere up to one minute. A mass loss of one percent is therefore not unexpected, but the mass loss of almost 9 wt% is far higher. This means that some part of the drying process did not function as intended and that the figure of 10.8 wt% nonfreezing water is not accurate.

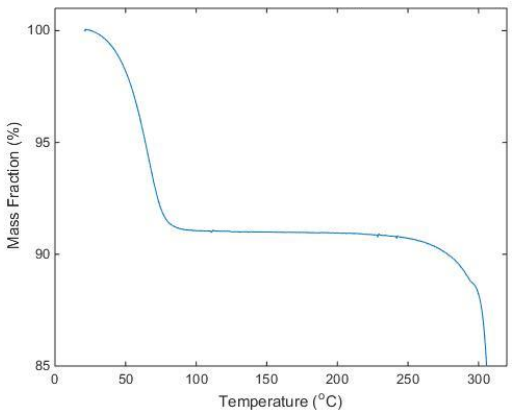

Figure 37. TGA scan of dried β-cyclodextrin with higher than expected water content.

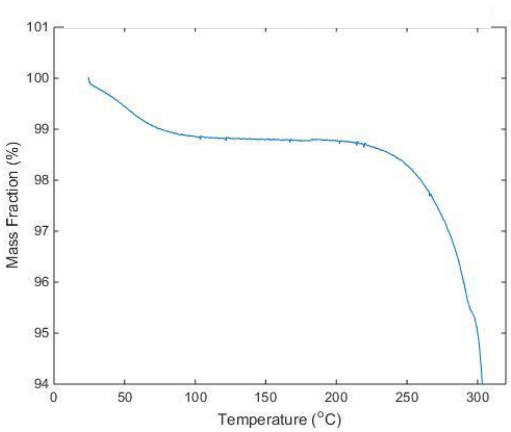

Figure 38. TGA scan of dried β-cyclodextrin with typical weight loss.

4.2.4. Phase Diagram

The data obtained by sorption calorimetry, DVS and DSC was used to derive the phase diagram seen in Figure 39. S_1 to S_3 is designating the different solid crystal forms of β-cyclodextrin. The DVS data at 25-50 °C marking the one-phase region for S_2 were too imprecise to accurately represent the transition. The sorption calorimetry data for 75 mg was not used, as it was not in accordance with the other two sorption calorimetry and the DSC measurements. No thermally induced transitions could be found in the S_1-S_3 region, and the non-freezing water was set at 15.8 wt% based on Figure 36. The liquidus line appears linear between 15 and 40 wt% water, but it would be beneficial to study it with more sensitive methods at lower cyclodextrin concentrations, in order to increase the accuracy of the liquidus line in the region 2-15 wt% water. The DVS measurements clearly show that the two-phase regions for S_1-S_3 are steadily increasing in the range 25 to 60 °C. Higher temperatures were not tested in order to not damage the DVS equipment, but it would be beneficial for the phase diagram to create sorption isotherms at even higher temperatures.

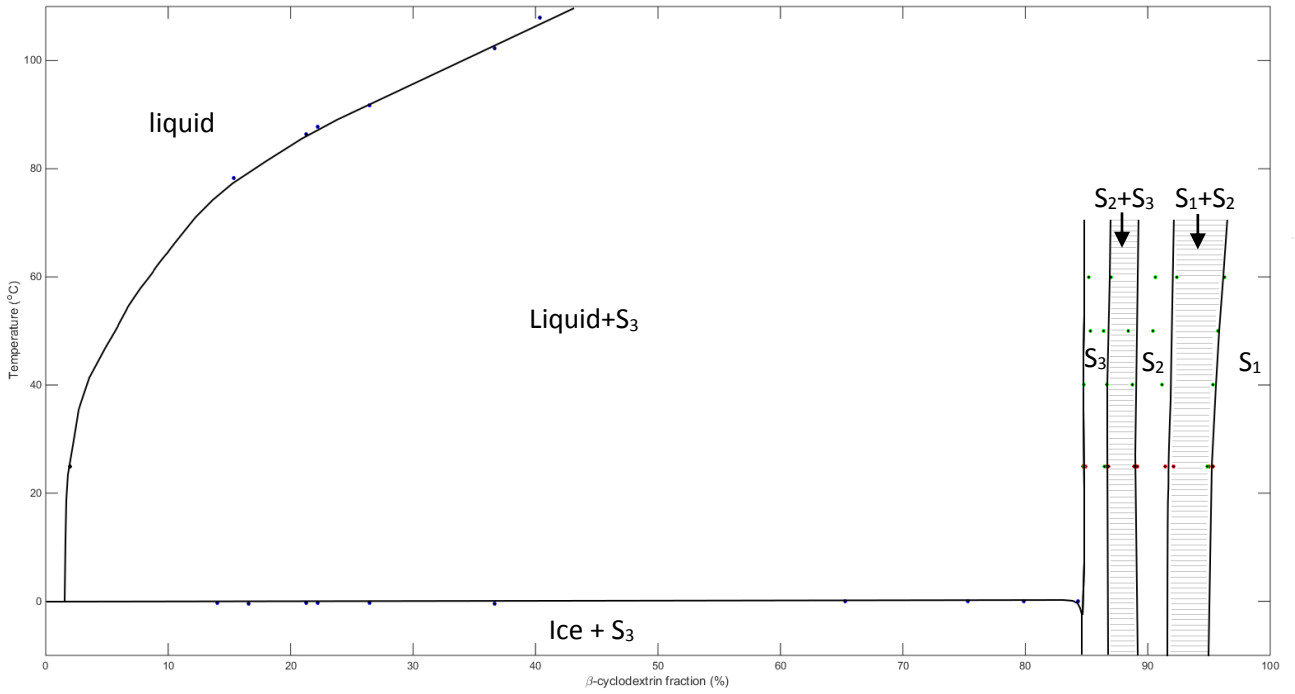

Figure 39. Temperature-composition phase diagram for the β-cyclodextrin/water system. Blue is DSC data, green is DVS data data, red is sorption calorimetry data and Black is literature data for β-cyclodextrin at 25 °C (Jozwiakowski 1985).

4.3 γ-cyclodextrin

4.3.1. Sorption Calorimetry

The sorption calorimetry measurement of γ-cyclodextrin (Figure 40) shows three possible one-phase regions in the range 0 to 13 %RH, 15 to 65 %RH and 75 to 95 %RH.

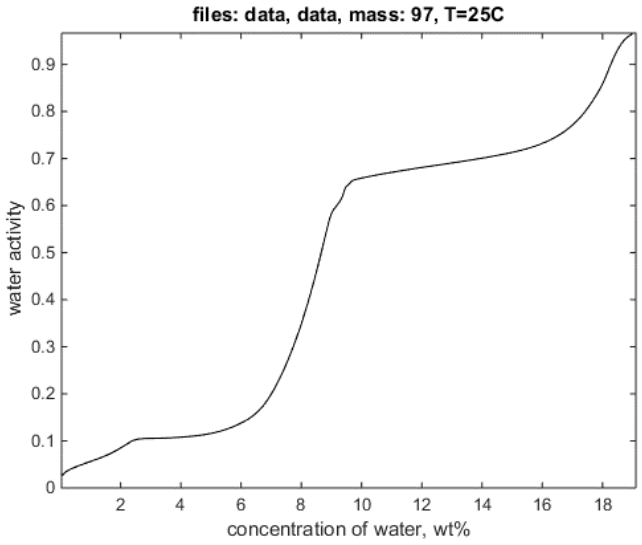

Figure 40. Sorption calorimetry of 80 mg γ-cyclodextrin.

4.3.2. X-Ray Diffraction

Upon closer analysis of the γ-cyclodextrin XRD data, it was possible to detect several possible transitions. The material also appeared to be significantly less crystalline with a lower signal-to-noise ratio than its α and β counterpart, leading to more difficulties comparing diffraction patterns. The first solid state transition was detected in sorption calorimetry between 12 and 15 %RH, and a corresponding diffraction pattern shift can be seen between γ-cyclodextrin equilibrated at 11.3 %RH and 21.6 %RH, as seen in Figure 41.

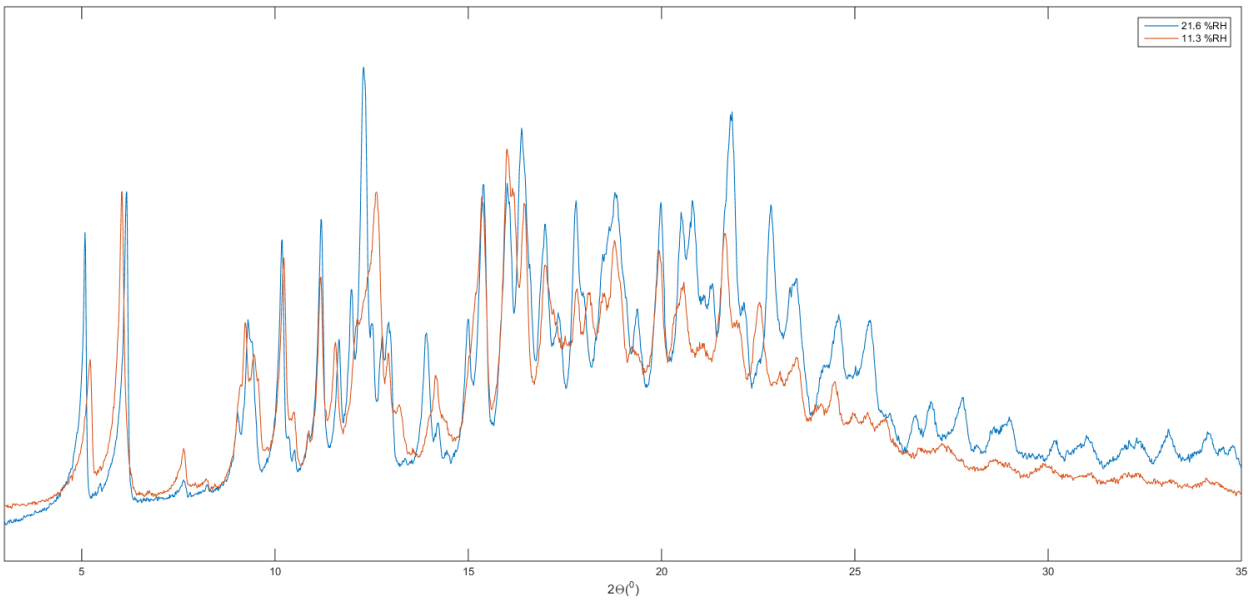

Figure 41. X-Ray diffraction patterns for γ-cyclodextrin equilibrated in 11.3 and 21.6 %RH.

The second noticeable shift in diffraction pattern is observed between γ-cyclodextrin equilibrated at 57.5 %RH and 70.9 %RH, as can be seen in Figure 42. Notable differences include additional peaks around 5°, 8°, 11°. and between 14 and 15°.

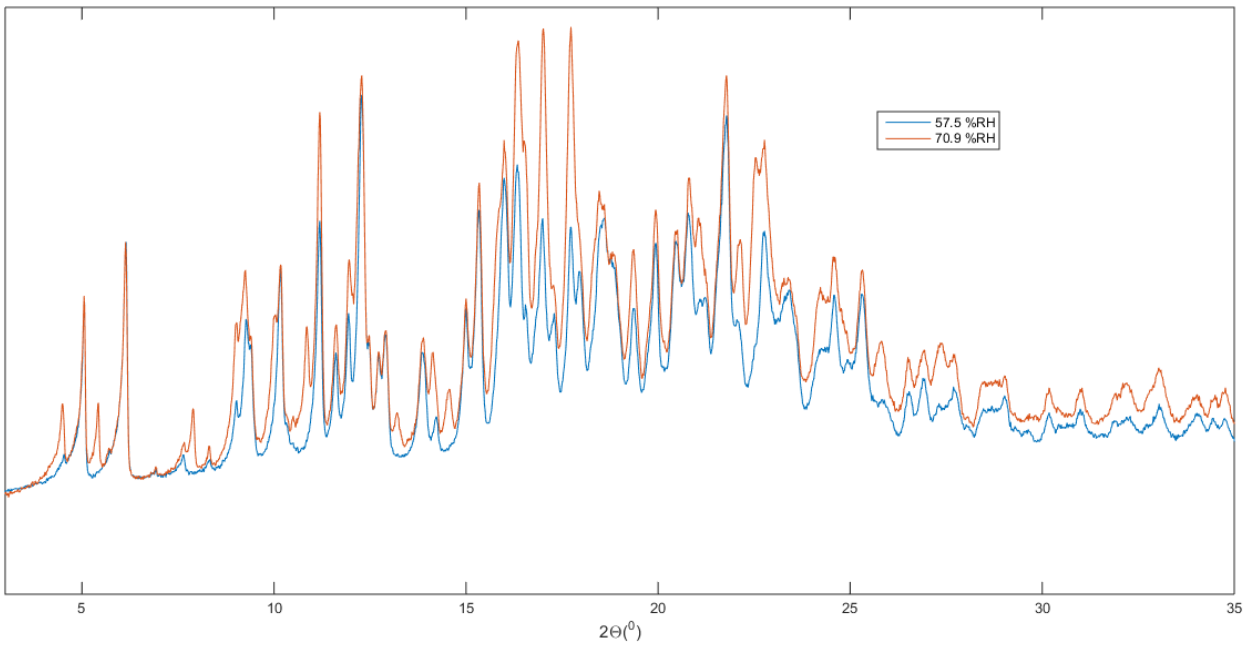

Figure 42. X-Ray diffraction patterns for γ-cyclodextrin equilibrated in 57.5 and 70.9 %RH.

A third solid state transition was found between 80.9 and 97.3 %RH (see Figure 43). Unlike the earlier transitions there is not a clear explanation from the sorption calorimetry experiment. This material, however, appears to be a lot more crystalline than the earlier diffraction patterns with a more distinct baseline.

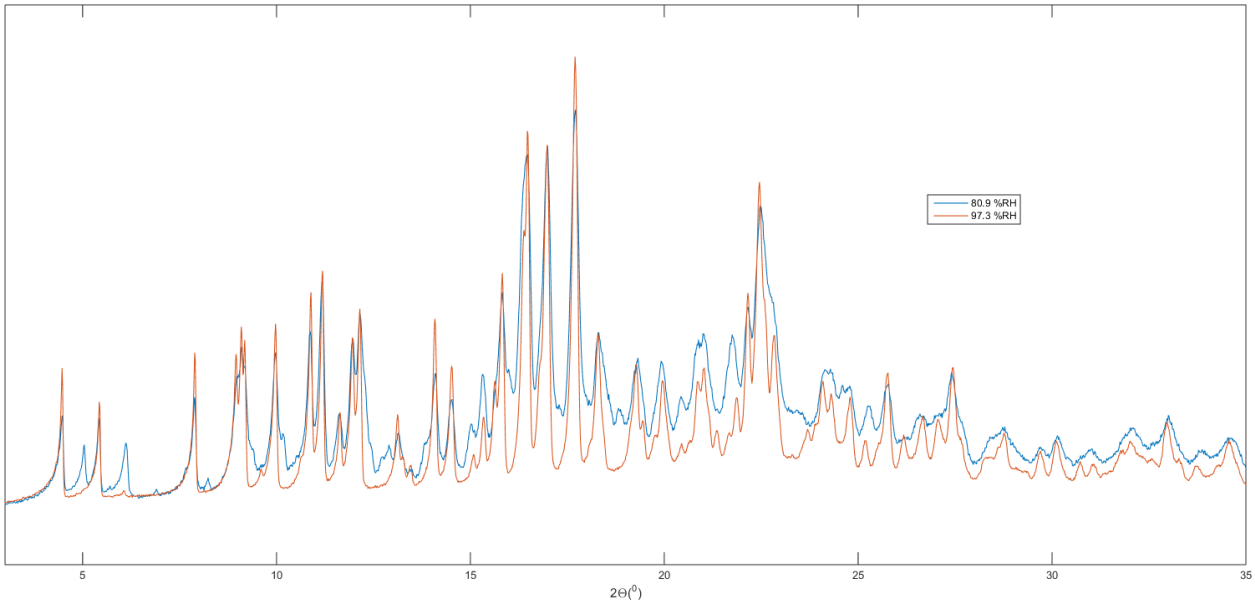

Figure 43. X-Ray diffraction patterns for γ-cyclodextrin equilibrated 80.9 and 97.3 %RH.

4.4. Inaccuracies and Improvements

As is the case in many areas, learning happens gradually. As the β-cyclodextrin was studied at an earlier time, the DSC methods used for α-cyclodextrin were better suited and more accurate than the saturated salt equilibration and addition of small amounts of water used for the β-cyclodextrin. The handling and storage of the highly hygroscopic cyclodextrins were also continuously improved, as awareness of their quick absorption of water increased.

One constant source of error that is very difficult to eliminate entirely is the presence of small amounts of water. Any water remaining after the cyclodextrin is dried under vacuum with molecular sieves will transfer to the sorption calorimetry and DSC measurements, and the DSC relies on drying the material at a slightly elevated temperature under a flow of dry nitrogen. While the vacuum method is generally reliable, there are exceptions such as the one seen in Figure 35, and the DSC method definitely leaves some water as is evident from comparing the results to sorption calorimetry, and Figure 38 where TGA shows a mass loss until over 100 °C.

4.5. Future Research

The natural progression for this thesis would be to study the phase behavior of γ-cyclodextrin in as much detail as α-cyclodextrin. The sorption calorimetry and XRD combined give an insight to the solid phase of γ-cyclodextrin, but additional DSC and DVS data could give additional understanding of the transitions, as well as provide information regarding dissolution, and other thermally induced transitions such as T_g and T_m for the different crystal structures or the amorphous state.

Other interesting methods that could provide useful data is the desorption calorimetry method (Kocherbitov 2004) where a salt solution is used to dehydrate a sample with high water activity. Since literature describes α-, and γ-cyclodextrin hydrates that could not be found through the sorption calorimetry or vapor sorption measurements in this study it would be useful to measure the phase transition directly.

Lastly, it would be beneficial to characterize the multitude of transitions found in α-cyclodextrin to definitively understand the phase behavior at a given temperature and composition.

5. Conclusions

The structures of α-, β-, and γ-cyclodextrin at different temperatures and compositions were investigated with the help of sorption calorimetry, DSC, DVS, TGA and earlier X-ray diffraction patterns. For α-cyclodextrin the DVS, sorption calorimetry and X-ray data all pointed towards three distinct crystal structures in the range of 0 to 10 wt% water, with α-CD·6H_2O being found over a large humidity range over approximately 20 %RH. The DSC provided dissolution temperatures, $T_{m,ice}$ and several isothermal transitions over 55 wt% cyclodextrin, which could in turn create a phase diagram for α-cyclodextrin with four separate crystal structures.

The β-cyclodextrin crystal structures mirrored the α-cyclodextrin in the region up to 15 wt% water, with sorption calorimetry, DVS and X-ray data verifying three distinct crystal structures. Unlike α-cyclodextrin there were no thermally induced phase changes in the solid region, and the dissolution temperature was far higher. A phase diagram could be constructed for β-cyclodextrin, with fewer distinct phases than α-cyclodextrin.

While a phase diagram could not be constructed due to a focus on α- and β-cyclodextrin, a comparison of sorption calorimetry and X-ray diffraction patterns detected three separate structures, with a fourth being indicated by the diffraction pattern for 97.3 %RH. The diffraction patterns, however, were less orderly than the other cyclodextrin patterns indicating that γ-cyclodextrin may be more amorphous at lower humidity levels than the other first-generation cyclodextrins.

6. Literature Cited

Askeland, D. R. (**2014**). *Essentials of materials science and engineering*. 3. ed. SI Stamford, CT: Cengage Learning.

Betzel, C.; Saenger, W.; Hingerty, B. E.; Brown, C. M. (1984). Topography of cyclodextrin inclusion complexes. Part 20. Circular and flip-flop hydrogen bonding in β-cyclodextrin undecahydrate: a neutron diffraction study. *J. Am. Chem. Soc. 106*, 7545.

Coats, A. W.; Redfern, J. P. (**1963**). Thermogravimetric analysis. A review. *Analyst*. 88, 906-924.

Fried, J. R. (**2003***). Polymer science and technology*. 2. ed. Upper Saddle River, N.J.: Prentice Hall PTR.

Harata, K. (**1984**). Crystal Structure of γ-Cyclodextrin at Room Temperature. *Chem. Lett***.** 641-644.

Harata, K. (**1987**). The Structure of the Cyclodextrin Complex. XX. Crystal Structure of Uncomplexed Hydrated γ-Cyclodextrin. *Bull. Chem. Soc. Jpn*. *60*, 2763-2767.

Jozwiakowski, M. J.; Connors, K. A. (**1985**). Aqueous solubility behaviour of three cyclodextrins. *Carbohydr. Res*. 143, 51-59.

Klar, B.; Hingerty, B.; Saenger, W.; (**1980**). Topography of cyclodextrin inclusion complexes. XII. Hydrogen bonding in the crystal structure of α-cyclodextrin hexahydrate: the use of a multi-counter detector in neutron diffraction. *Acta Cryst*. B36, 1154-1165.

Kocherbitov, V.; L. Wadsö, A. (**2004**) Desorption Calorimetric Method for Use at High Water Activities. *Thermochimica Acta*. 411(1): p. 31-36.

Kocherbitov, V.; Alfredsson, V. (**2011**). Assessment of Porosities of SBA-15 and MCM-41 Using Water Sorption Calorimetry. *Langmuir.* 27(7), 3889-3897.

Kocherbitov, V. (**2016**). The nature of nonfreezing water in *Carbohydr. Polym*. Carbohydrate Polymers. 150, 353-358.

Lindner, K.; Saenger, W. (**1982**). Crystal and molecular structure of cyclohepta-amylose dodecahydrate. *Carbohydr. Res.* 99(2), 103-115

Maclennan, J.M.; Stezowski, J. J. (**1980**). The crystal structure of uncomplexed-hydrated cyclooctaamylose. *Biochem. Biophys. Res. Comm*. 92(3), 926-932.

Manor, P. C.; Saenger*, W. (**1974**)*. Topography of cyclodextrin inclusion complexes. III. Crystal and molecular structure of cyclohexaamylose hexahydrate, the water dimer inclusion complex. *J. Am. Chem. Soc.* 96(11), 3630-3639

Martin Del Valle, Eva M. (**2004**). Cyclodextrin and their uses: a review. *Process Biochem.* 39(9), 1033-1046.

Nakai, Y.; Yamamoto, K.; Terada, K.; Kajiyama, A.; Sasaki I. (**1986**). Properties of Crystal Water of α-, β-, and γ-Cyclodextrin. *Chem. Pharm. Bull.* 34(5), 2178-2182

Puliti, R.; Mattia, C. A.; Paduano, L. (**1998**). Crystal structure of a new alpha-cyclodextrin hydrate form. Molecular geometry and packing features: disordered solvent contriubution. *Carbohydr. Res*. 310(1-2), 1-8.

Ripmeester, J. A. (**1993**). Crystalline β-cyclodextrin hydrate is non-stochiometric with 10.5-12 waters per cyclodextrin molecule. *Supramol. Chem*. *2*, 89-91.

Saenger, W.; Jacob, J; Gessler, K.; Steiner, T.; Hoffmann, D.; Sanbe, H.; Koizumi, K.; Smith, S. M.; Takaha, T.; (**1998**). Structures of the Common Cyclodextrins and Their Larger Analogues – Beyond the Doughnut. *Chem. Rev.* 98(5), 1787-1802.

Sheokand, S.; Modi, S. R.; Bansal, A. K. (**2014**). Dynamic Vapor Sorption as a Tool for Characterization and Quantification of Amorphous Content in Predominantly Crystalline Materials. *J. Pharm. Sci*. 103(11), 3364-3376.

Specogna, E.; Li, K. W.; Djabourov, M.; Carn, F.; Bouchemal, K. (**2015**). Dehydration, Dissolution and Melting of Cyclodextrin Crystals. *J. Phys. Chem. B*. 119(4), 1433-1442.

Steiner, T.; Koellner, G. (**1994**). Crystalline β-Cyclodextrin Hydrate at Various humidities: Fast, Continuous and Reversible Dehydration Studied by X-ray Diffraction. *J. Am. Chem. Soc*. 116(12), 5122-5128.

Szejtli, J. (**1998**). Introduction and General Overview of Cyclodextrin Chemistry. *Chem. Rev*. 98(5), 1743-1754.

Wadsö, L.; Markova, N. (**2002**). A method to simultaneously determine sorption isotherms and sorption enthalpies with a double twin microcalimeter. *Rev. Sci. Instrum.* 2002, 73(7), 2743-2754.

7. Appendices

7.1 α-cyclodextrin data

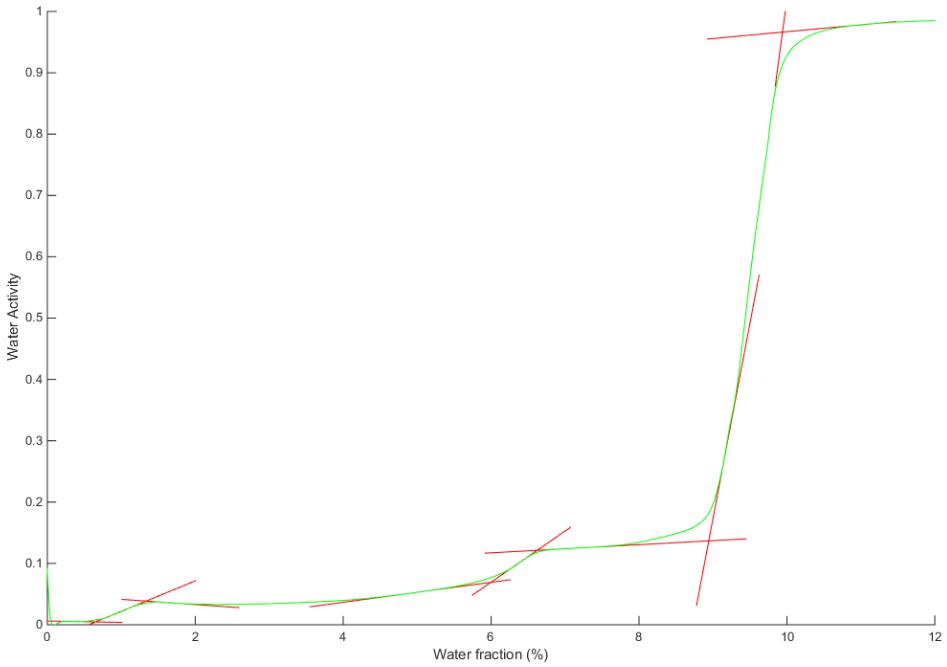

Figure 44. An illustration for the calculation of the sorption calorimetry phase transitions

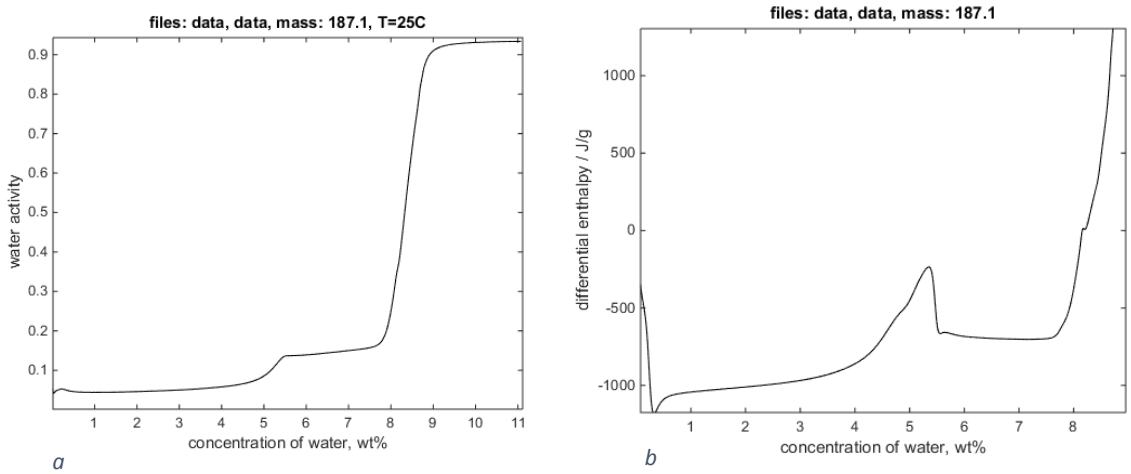

Figure 45. Less precise sorption calorimetry measurement of (a) the sorption isotherm on α-cyclodextrin and (b) the corresponding differential enthalpy

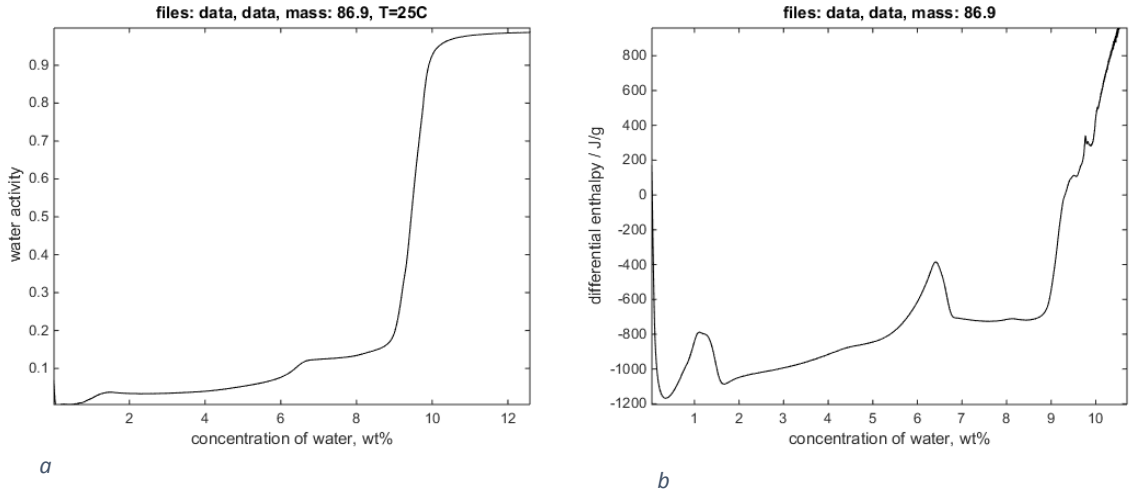

Figure 46. Sorption calorimetry measurement of (a) the sorption isotherm on α-cyclodextrin and (b) the corresponding differential enthalpy

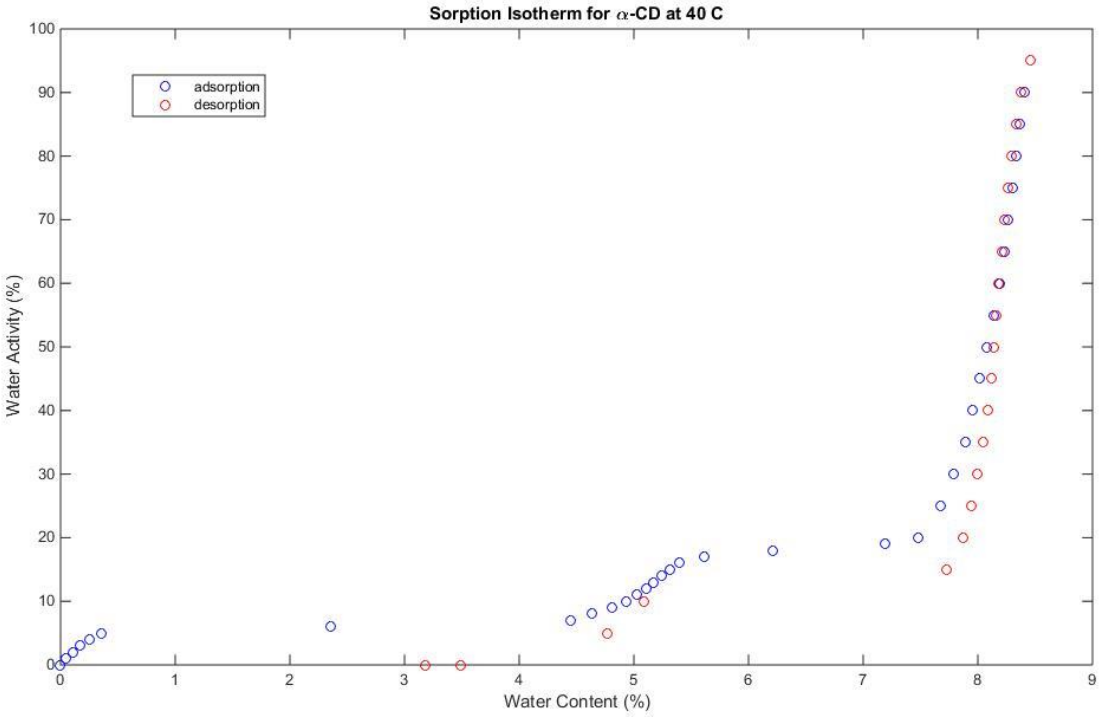

Figure 47. Sorption isotherm of α-cyclodextrin from DVS measurements at 40 °C

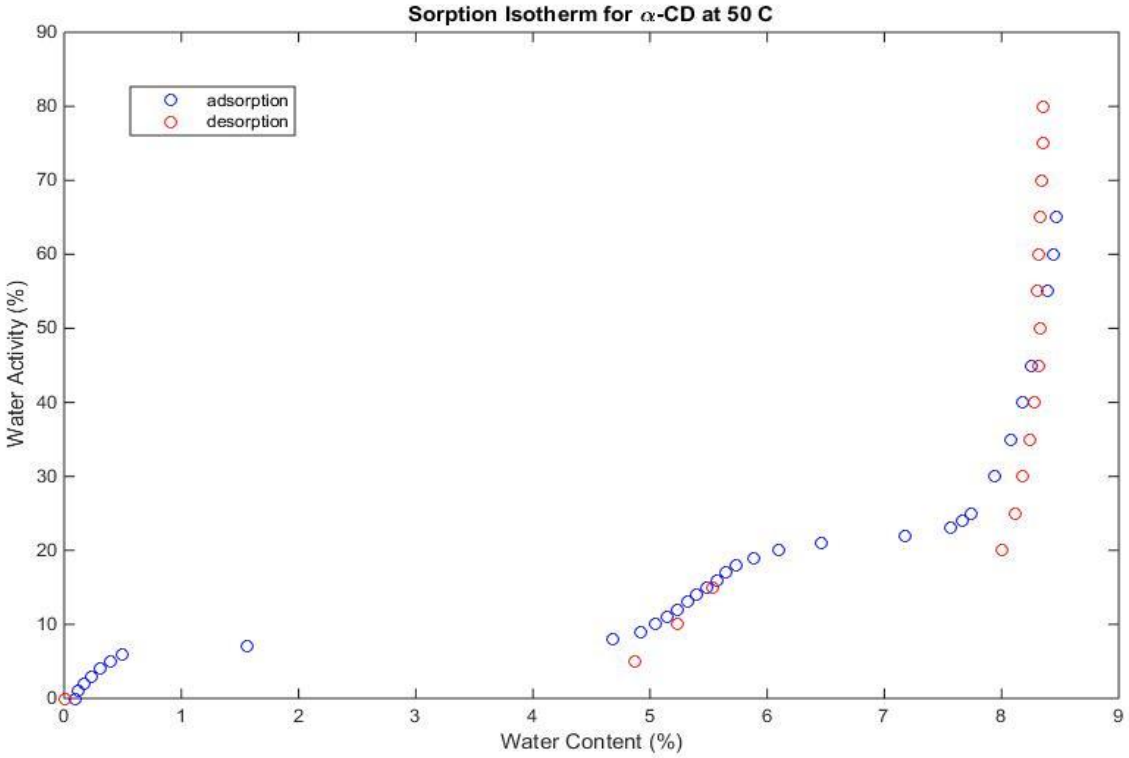

Figure 48. Sorption isotherm of α-cyclodextrin from DVS measurements at 50 °C

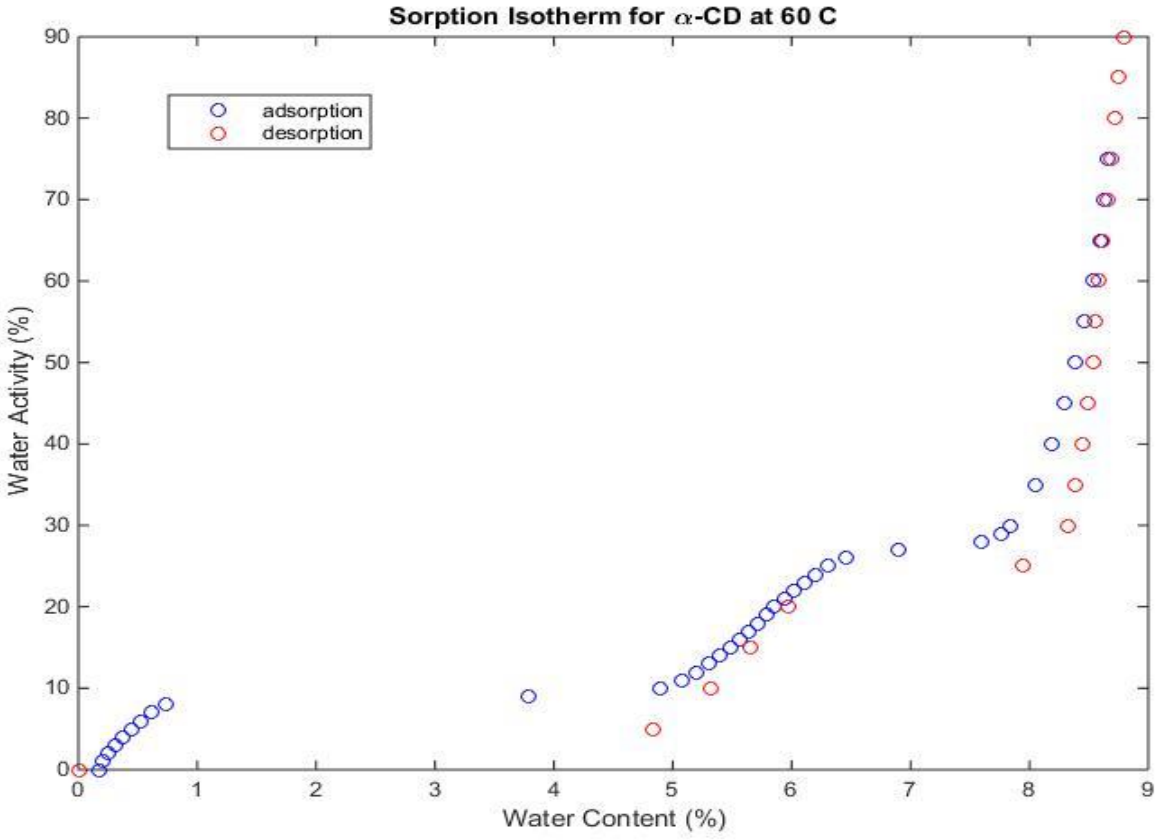

Figure 49. Sorption isotherm of α-cyclodextrin from DVS measurements at 60 °C

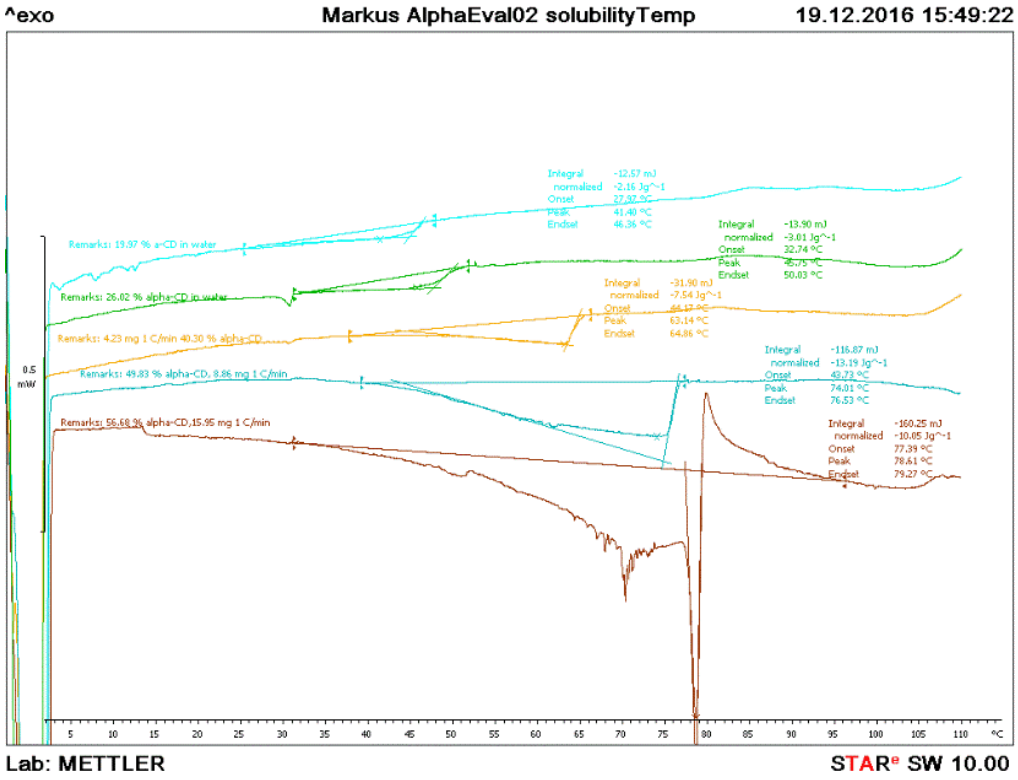

Figure 50. DSC measurements of α-cyclodextrin between 20.0 wt% CD and 56.7 wt% CD.

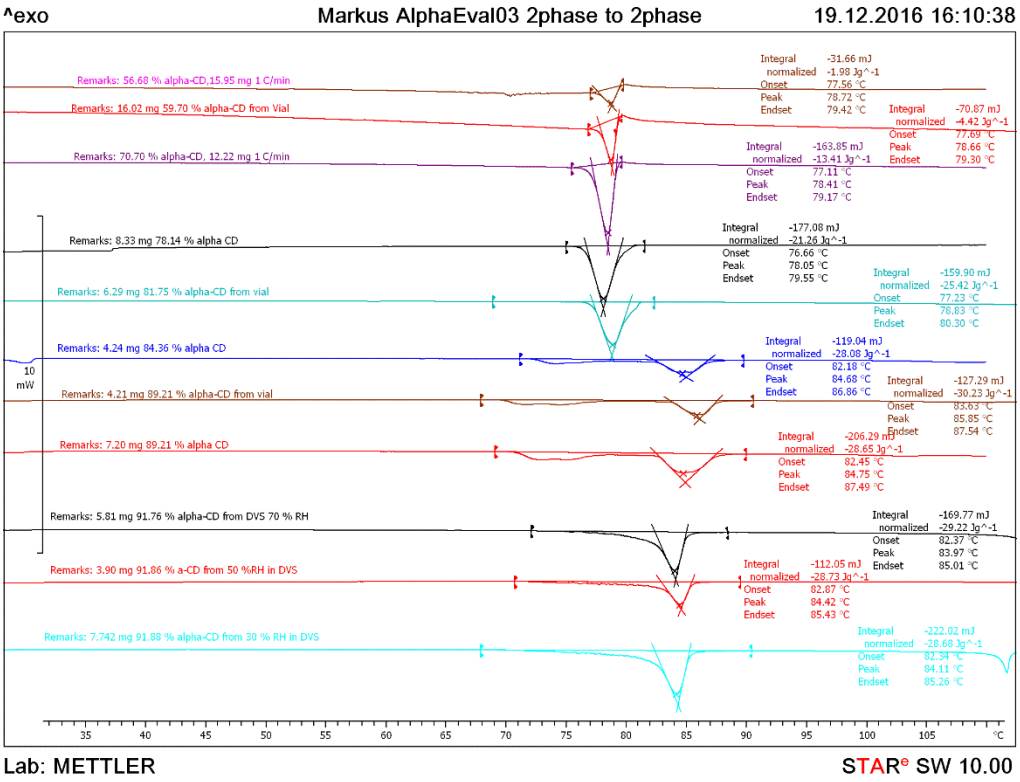

Figure 51. DSC measurements of α-cyclodextrin between 56.7 wt% CD and 91.9 wt% CD.

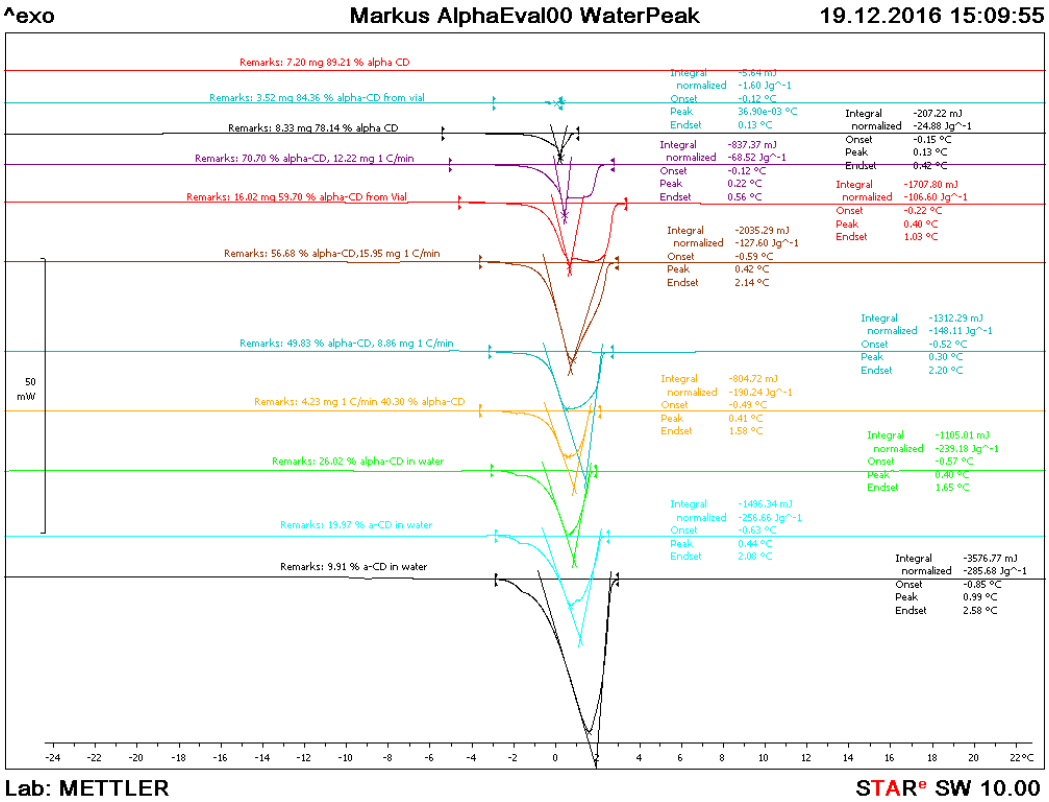

Figure 52. DSC measurements of α-cyclodextrin between 9.9 wt% CD and 89.2 wt% CD.

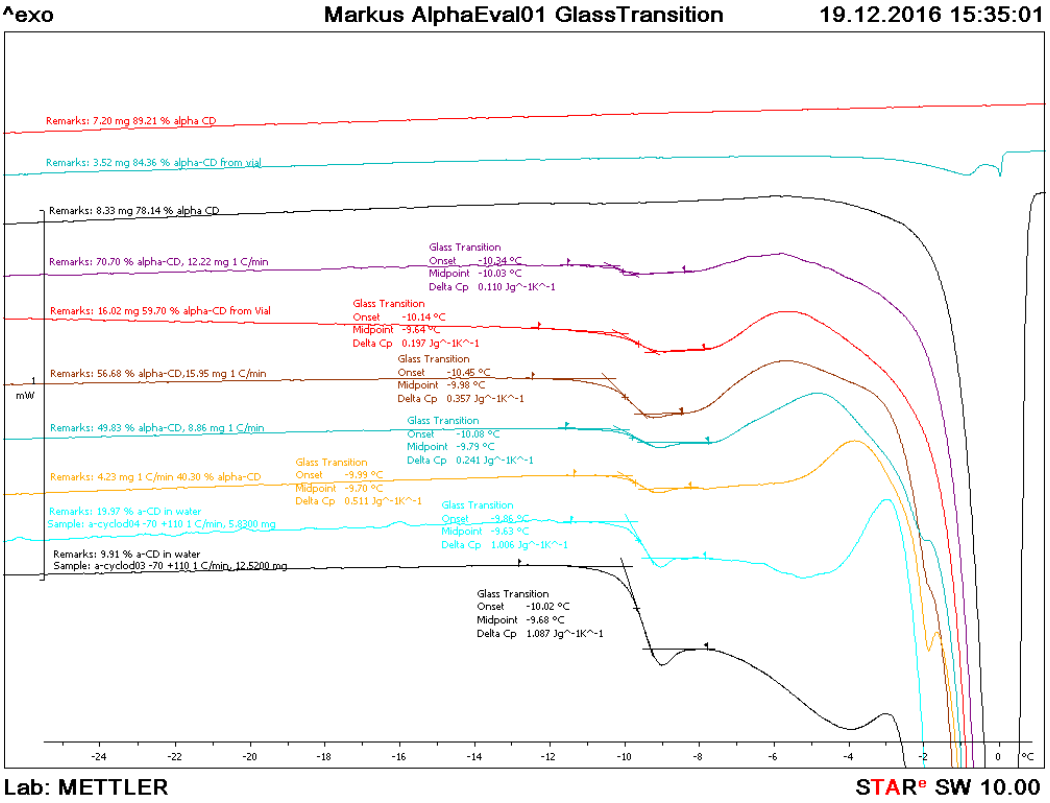

Figure 53. DSC measurements of α-cyclodextrin between 9.9 wt% CD and 89.2 wt% CD.

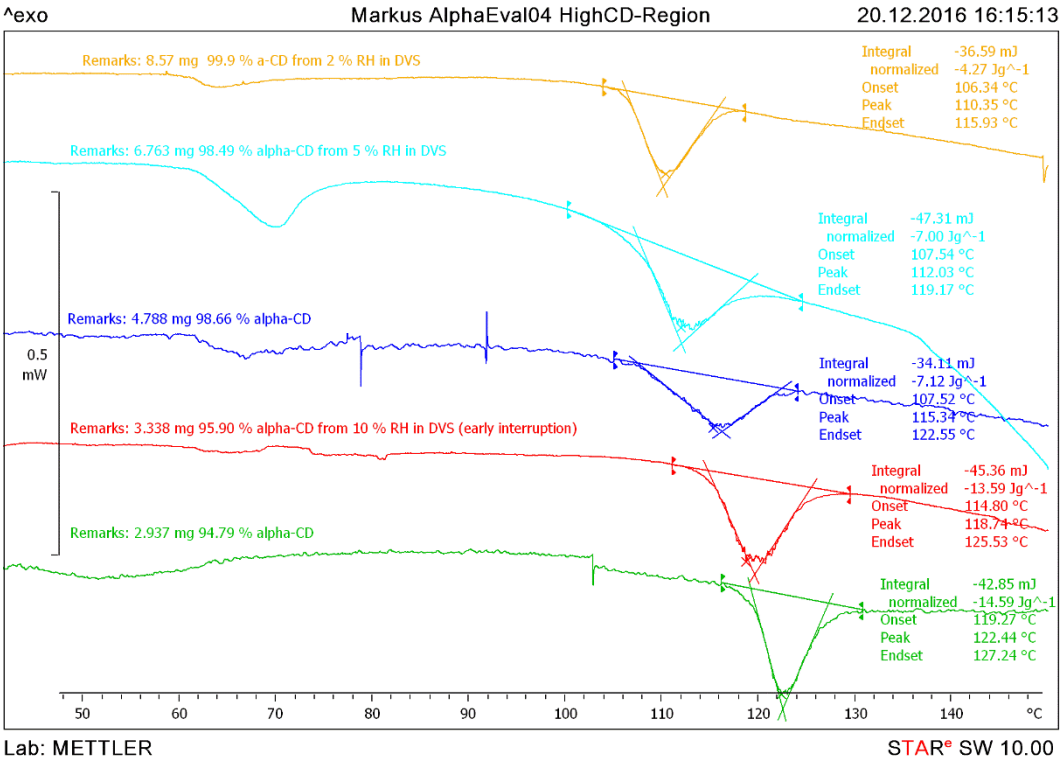

Figure 54. DSC measurements of α-cyclodextrin between 94.8 wt% CD and 99.9 wt% CD.

7.2 β-cyclodextrin data

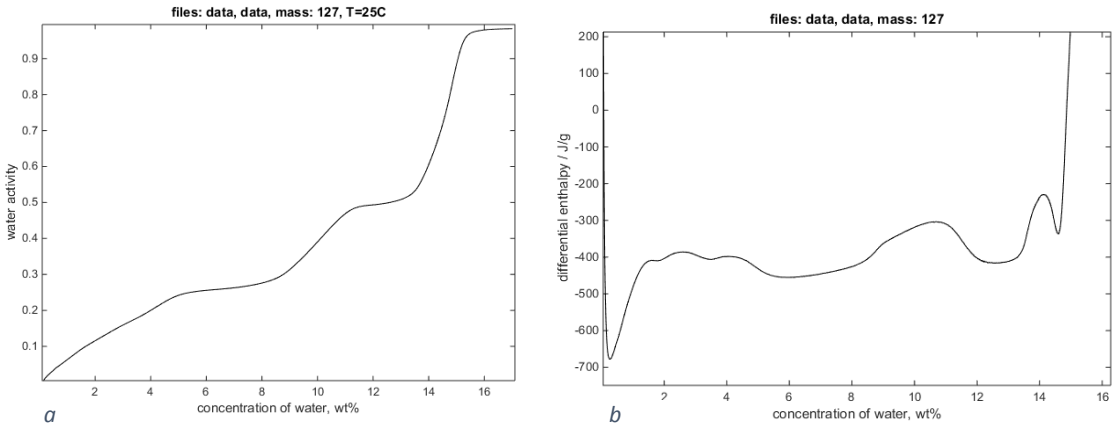

Figure 55. Sorption calorimetry measurement of (a) the sorption isotherm on β-cyclodextrin and (b) the corresponding differential enthalpy

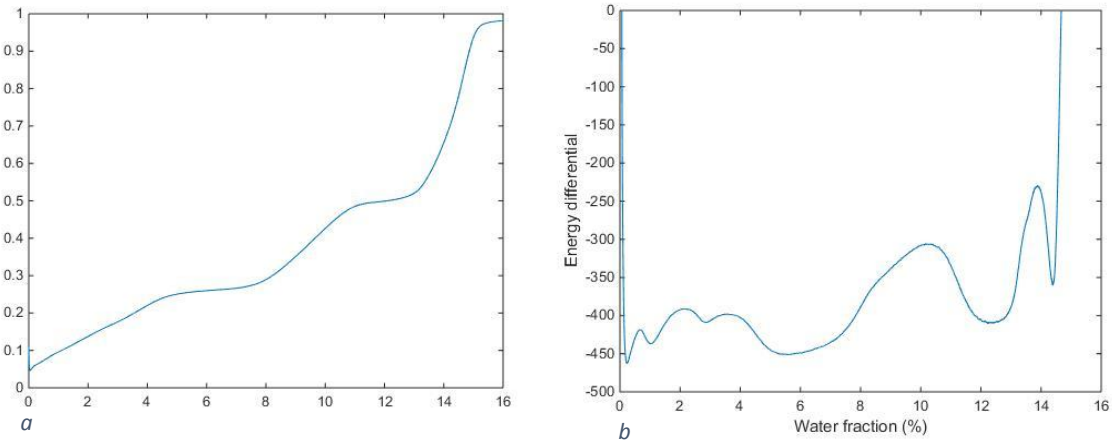

Figure 56. Sorption calorimetry measurement of (a) the sorption isotherm on β-cyclodextrin and (b) the corresponding differential enthalpy

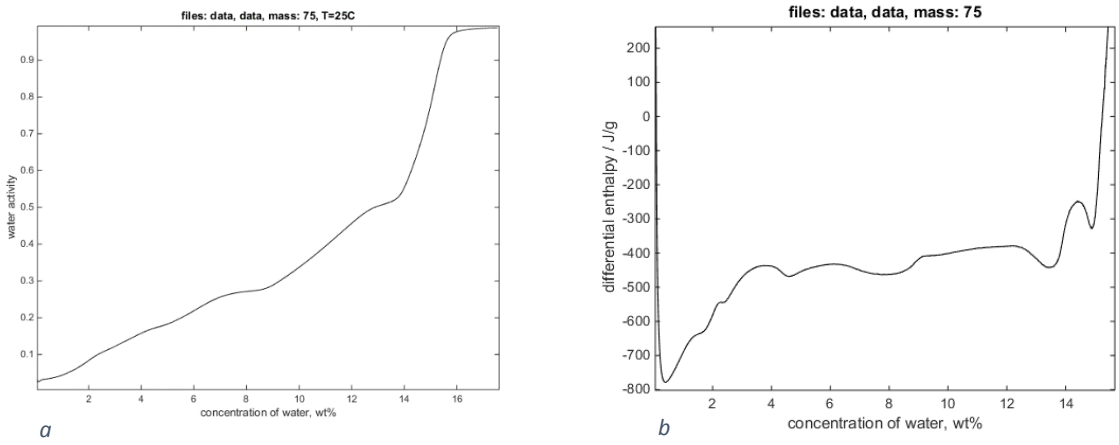

Figure 57. Sorption calorimetry measurement of (a) the sorption isotherm on β-cyclodextrin and (b) the corresponding differential enthalpy

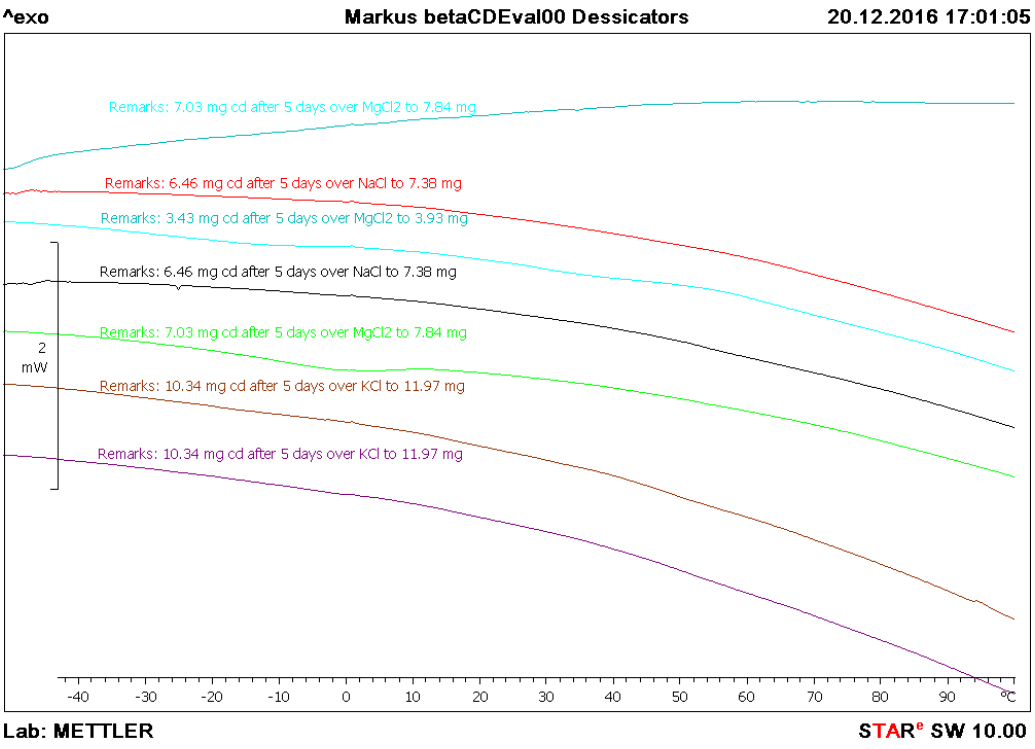

Figure 58. Primary and secondary DSC measurements of β-cyclodextrin equilibrated over saturated salt solutions.

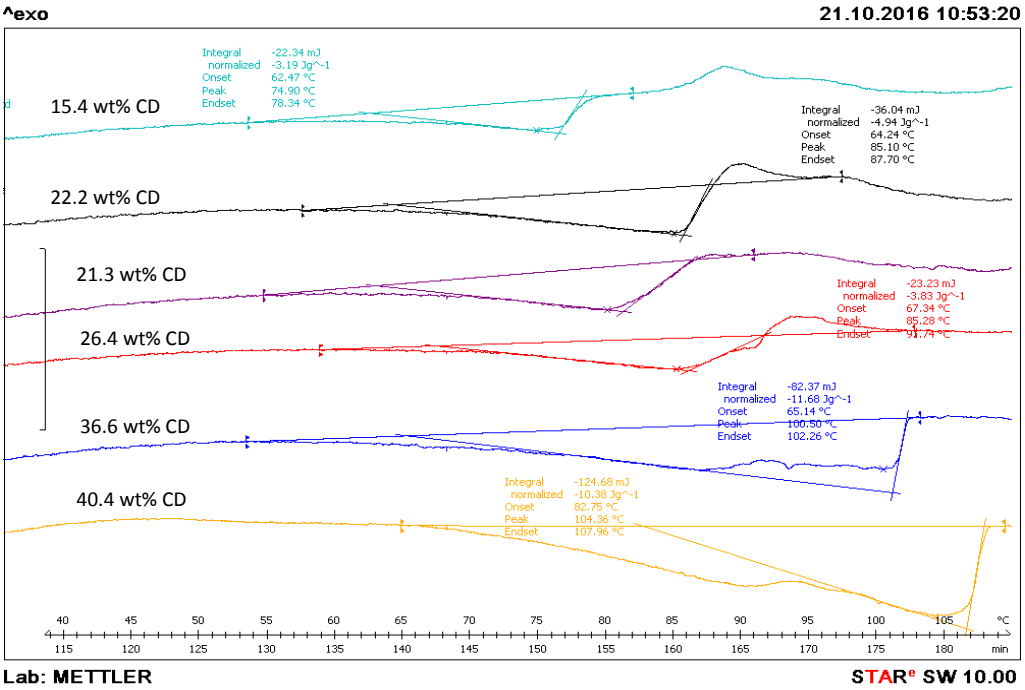

Figure 59. DSC measurements of β-cyclodextrin in the range of 40 to 110 degrees celsius

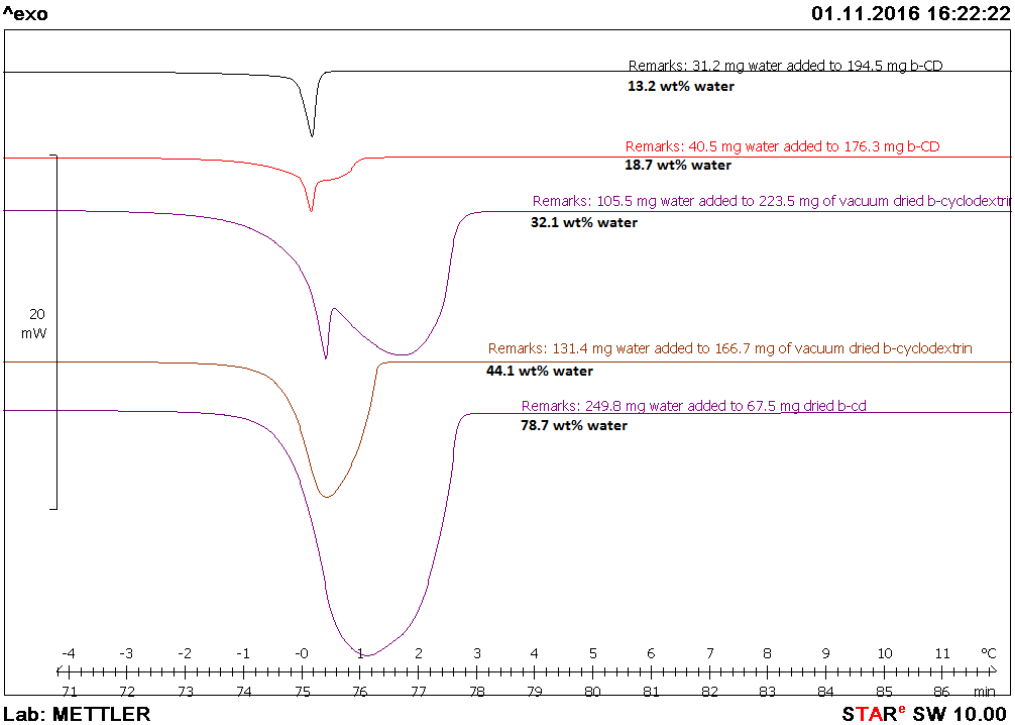

Figure 60. Some DSC scans of β-cyclodextrin in the range -4 to +11 degrees Celsius. Samples prepared by mixing dried cyclodextrin and liquid water

7.3 γ-cyclodextrin data

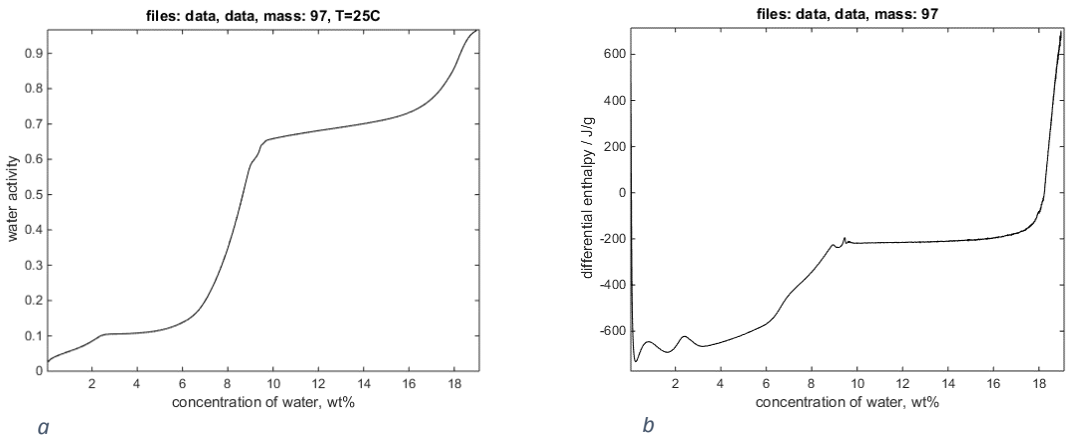

a *b*

Figure 61. Sorption calorimetry measurements of (a) the sorption isotherm on γ-cyclodextrin and (b) the corresponding differential enthalpy